Constraining Scalar Field Dark Matter scenarios with Gravitational Lensing

Raquel Galazo-García
Collaborators: Eric Jullo, Marceau Limousin, Emmanuel Nezri

Laboratoire d'Astrophysique de Marseille
European Physical Society Conference on High Energy Physics
Marseille, July 9, 2025

What we know about dark matter

The standard cosmological model, ΛCDM → **DM is described as a cold DM fluid.**

- **27% of the energy density of the universe.**
- **Dark** (transparent): no/weakly electromagnetic interactions.
- **Collisionless**: no/weakly self-interaction or interaction with baryons
- **Cold** (non-relativistic): moves much slower than c.
- **Pressureless:** gravitational attractive, clusters.

Energy content of the Universe

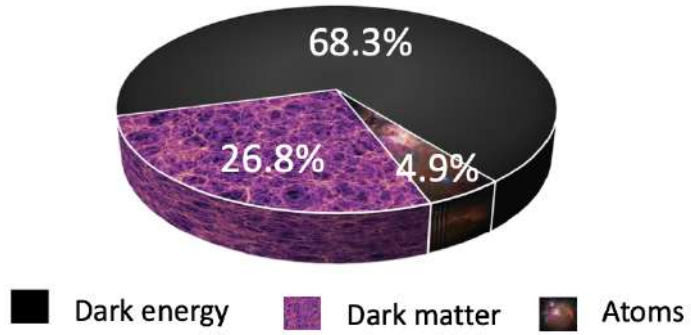

However, we remain ignorant about its basic properties for example the mass.

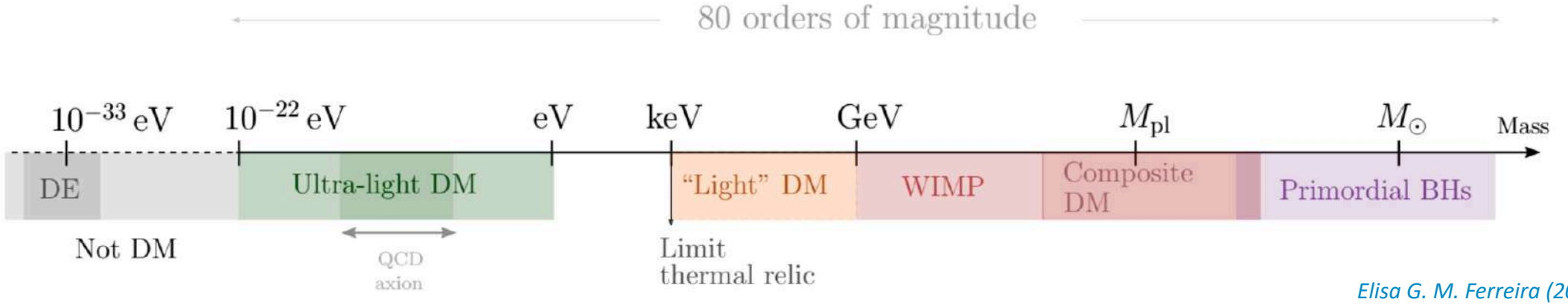

Elisa G. M. Ferreira (2020)

What we know about dark matter

The standard cosmological model, ΛCDM → **DM is described as a cold DM fluid.**

- **27% of the energy density of the universe.**
- **Dark** (transparent): no/weakly electromagnetic interactions
- **Collisionless**: no/weakly self-interaction or interaction with baryons
- **Cold** (non-relativistic): moves much slower than c.
- **Pressureless:** gravitational attractive, clusters.

Energy content of the Universe

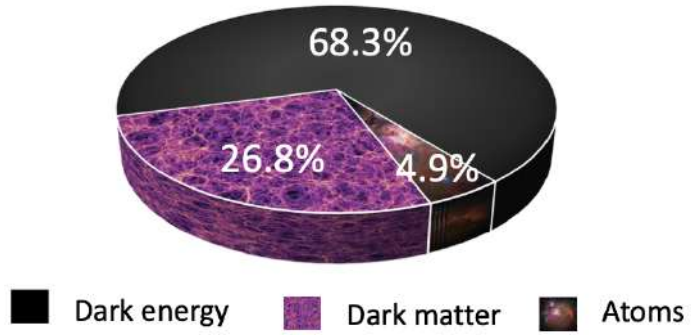

However, we remain ignorant about its basic properties for example the mass.

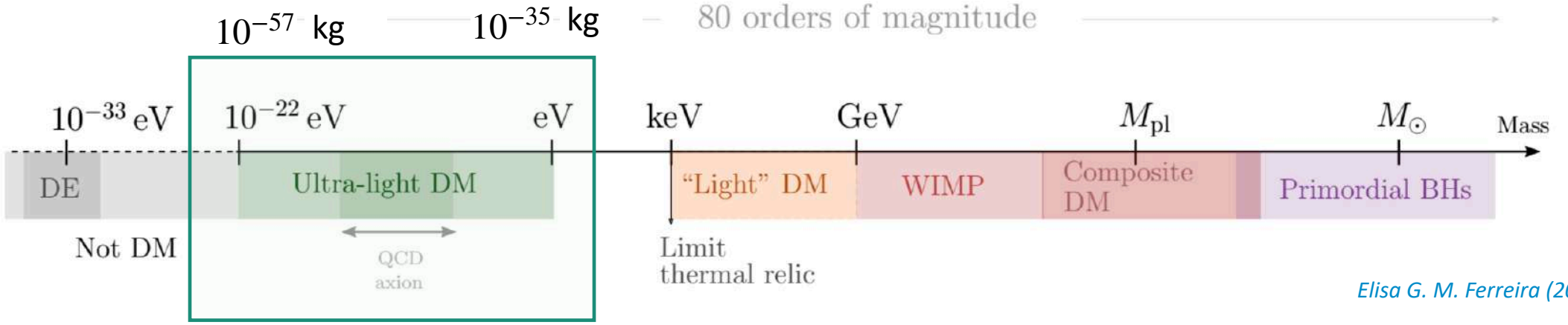

Elisa G. M. Ferreira (2020)

Scalar Field Dark Matter (SFDM) at small scales

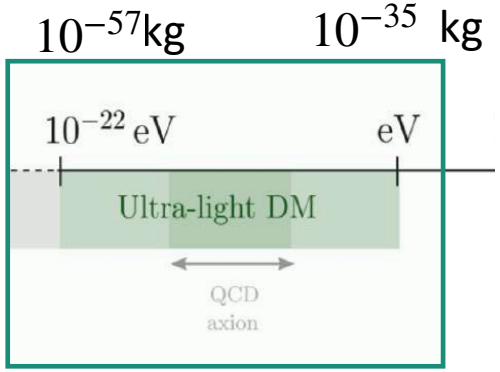

Because of its ultra-light mass → Large de Broglie wavelength, $\lambda_{dB} \sim 1/mv$

- λ_{dB}~ pc — kpc
- Small scales: wavelike behaviour.
- **Solitons**: stable equilibrium configurations → **Flat density profile at the center of the halos.**

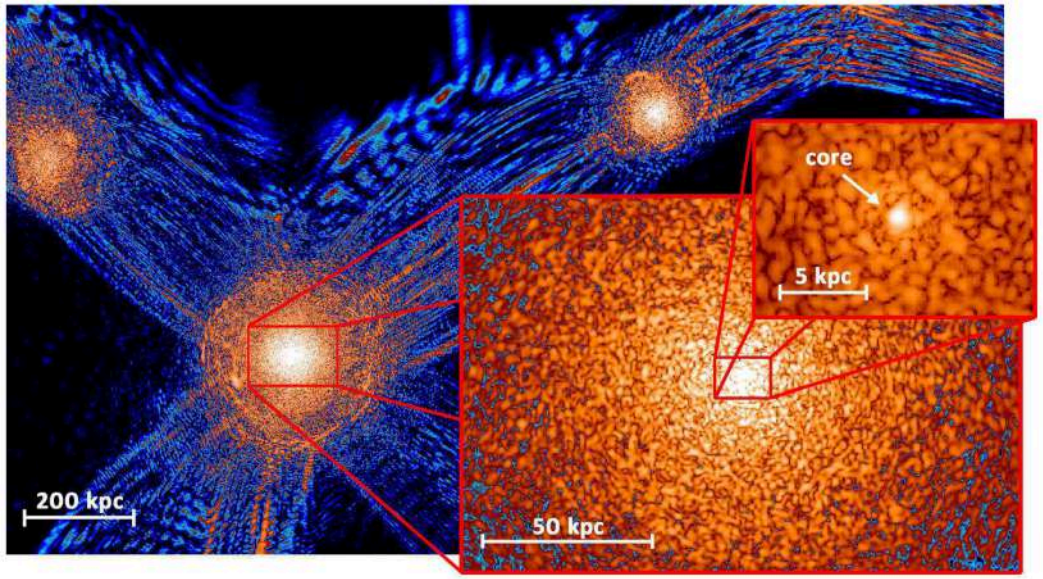

A slice of density field of ψDM simulation on various scales at z=0.1

Schive, Chiueh, and Broadhurst (2014)

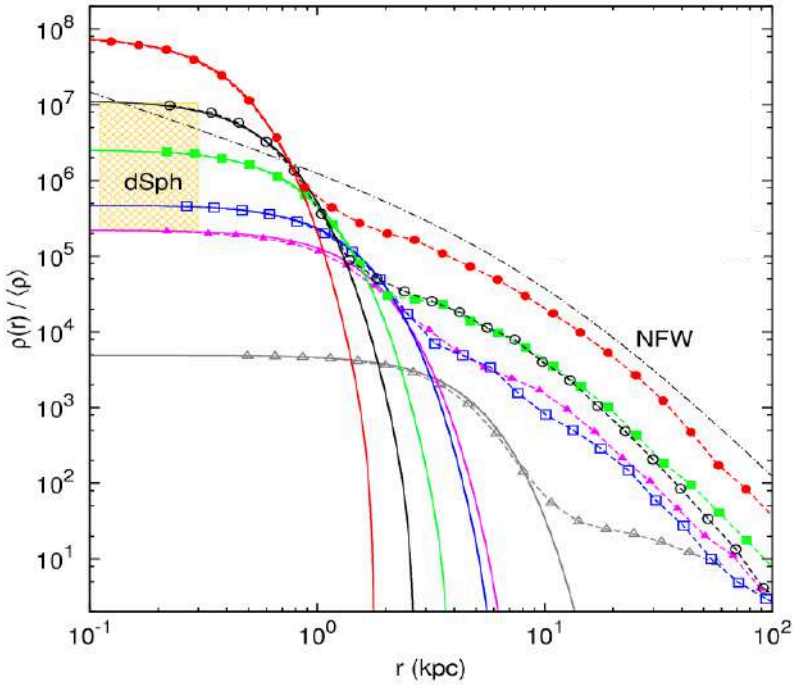

Radial density profiles of haloes formed in the ψDM model

SFDM at large scale scales

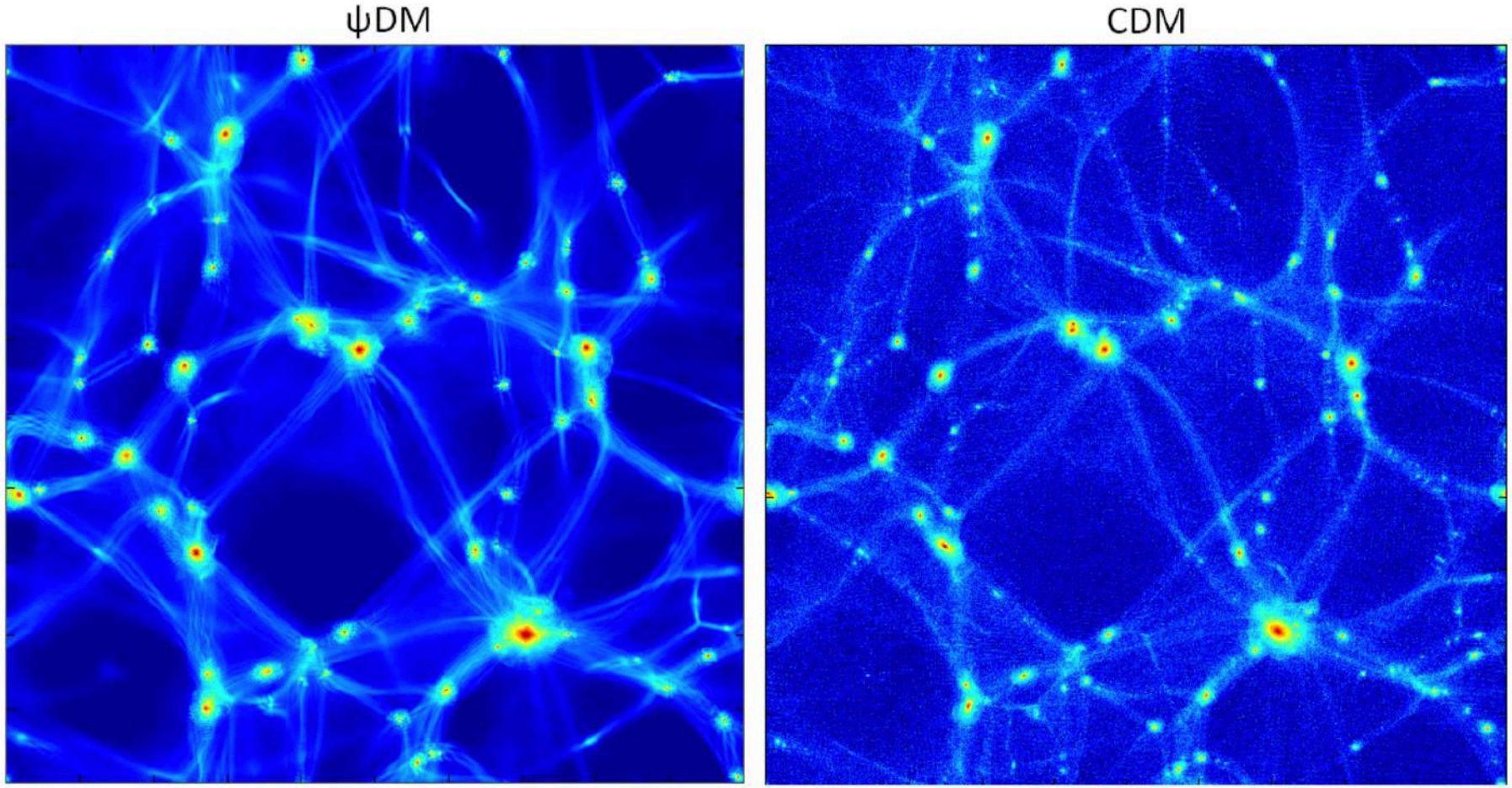

SFDM Recover CDM large scale distribution of filaments and voids

Schive, Chiueh, and Broadhurst (2014)

SFDM model

DM is represented by a **scalar field minimally coupled to gravity** given by the Lagrangian:

$$\mathcal{L}_\phi = -\frac{1}{2} g^{\mu\nu} \partial_\mu \phi \partial_\nu \phi - V(\phi),$$

The scalar field potential $V(\phi)$ must have a **parabolic minimum**

$$V(\phi) = \frac{m^2}{2}\phi^2 + V_I(\phi),$$

Fuzzy DM (FDM)

$$V_I(\phi) = 0.$$

m

Quartic model

$$V_I(\phi) = \frac{\lambda_4}{4}\phi^4,$$

m, λ_4

Repulsive → $\lambda_4 > 0$

SFDM model

DM is represented by a **scalar field minimally coupled to gravity** given by the Lagrangian:

$$\mathcal{L}_\phi = -\frac{1}{2} g^{\mu\nu} \partial_\mu \phi \partial_\nu \phi - V(\phi),$$

The scalar field potential $V(\phi)$ must have a **parabolic minimum**

$$V(\phi) = \frac{m^2}{2}\phi^2 + V_I(\phi),$$

Fuzzy DM (FDM)

$$V_I(\phi) = 0.$$

m

Quartic model

$$V_I(\phi) = \frac{\lambda_4}{4}\phi^4,$$

m, λ_4

Repulsive → $\lambda_4 > 0$

Non-relativistic dynamics for quartic self-interaction

FIELD PICTURE: SCHRÖDINGER—POISSON SYSTEM (SP)

$$i\frac{\partial\psi}{\partial t} = -\frac{1}{2m}\nabla^2\psi + m(\Phi_{\rm N} + \Phi_{\rm I})\psi,$$

Schrödinger equation (Gross—Pitaevskii)

$$\nabla^2\Phi_{\rm N} = 4\pi\mathcal{G}_{\rm N}\rho.$$

Poisson equation

Self-interactions (SI):

$$V_I(\phi) = \frac{\lambda_4}{4}\phi^4,$$

strength of the repulsive SI

$$\Phi_I = \frac{3\lambda_4}{4m^3}|\psi|^2.$$

Self-interaction potential

$$\rho = m\psi\psi^*.$$

Ultra-light scalar density

Non-relativistic dynamics of scalar field dark matter

Self-interactions (SI):

$$V_I(\phi) = \frac{\lambda_4}{4}\phi^4,$$

strength of the repulsive SI

SCHRÖDINGER—POISSON SYSTEM (SP)

$$i\frac{\partial\psi}{\partial t} = -\frac{1}{2m}\nabla^2\psi + m(\Phi_{\rm N} + \Phi_{\rm I})\,\psi,$$

Schrodinger equation (Gross—Pitaevskii)

$$\Phi_I = \frac{3\lambda_4}{4m^3}|\psi|^2.$$

Self-interaction potential

$$\nabla^2\Phi_{\rm N} = 4\pi\mathcal{G}_{\rm N}\rho.$$

Poisson equation

$$\rho = m\psi\psi^*.$$

Ultra-light scalar density

HYDRODYNAMICAL PICTURE

Madelung form $\psi \to \{\rho, S, \vec{v}\},$

$$\psi = \sqrt{\frac{\rho}{m}}\,e^{iS}, \quad \vec{v} = \frac{\nabla S}{m},$$

$$\frac{\partial\rho}{\partial t} + \nabla\cdot(\rho\vec{v}) = 0,$$

Continuity equation

$$\frac{\partial\vec{v}}{\partial t} + (\vec{v}\cdot\nabla)\vec{v} = -\nabla\left(\Phi_{\rm N} + \Phi_{\rm Q} + \Phi_{\rm I}\right).$$

Euler equation

$$\nabla^2\Phi_{\rm N} = 4\pi\mathcal{G}_{\rm N}\rho.$$

Poisson equation

Quantum pressure

$$\Phi_{\rm Q} = -\frac{\nabla^2\sqrt{\rho}}{2m^2\sqrt{\rho}}.$$

Non-relativistic dynamics of scalar field dark matter

Self-interactions (SI):

$$V_I(\phi) = \frac{\lambda_4}{4}\phi^4,$$

strength of the repulsive SI

SCHRÖDINGER—POISSON SYSTEM (SP)

$$i\frac{\partial\psi}{\partial t} = -\frac{1}{2m}\nabla^2\psi + m(\Phi_{\rm N} + \Phi_{\rm I})\,\psi,$$

Schrodinger equation (Gross—Pitaevskii)

$$\nabla^2\Phi_{\rm N} = 4\pi\mathcal{G}_{\rm N}\rho.$$

Poisson equation

$$\Phi_I = \frac{3\lambda_4}{4m^3}|\psi|^2.$$

Self-interaction potential

$$\rho = m\psi\psi^*.$$

Ultra-light scalar density

HYDRODYNAMICAL PICTURE

Madelung form $\psi \to \{\rho, S, \vec{v}\},$

$$\psi = \sqrt{\frac{\rho}{m}}\,e^{iS}, \quad \vec{v} = \frac{\nabla S}{m},$$

$$\frac{\partial\rho}{\partial t} + \nabla\cdot(\rho\vec{v}) = 0,$$

Continuity equation

$$\frac{\partial\vec{v}}{\partial t} + (\vec{v}\cdot\nabla)\vec{v} = -\nabla\left(\Phi_{\rm N} + \Phi_{\rm Q} + \Phi_{\rm I}\right).$$

Euler equation

$$\nabla^2\Phi_{\rm N} = 4\pi\mathcal{G}_{\rm N}\rho.$$

Poisson equation

Quantum pressure

$$\Phi_{\rm Q} = -\frac{\nabla^2\sqrt{\rho}}{2m^2\sqrt{\rho}}.$$

Soliton: hydrostatic equilibrium $\Phi_N + \Phi_I + \Phi_{\rm Q} = \alpha,$

Self-interacting soliton

Soliton: Hydrostatic equilibrium

$$\Phi_N + \Phi_I + \Phi_Q = \alpha,$$

Thomas-Fermi regime → $\Phi_Q \ll \Phi_I$

Soliton TF limit

$$\Phi_N + \Phi_I = \alpha,$$

Helmholtz equation:

$$\nabla^2\rho = -\frac{16\pi G m^4}{3\lambda_4}\rho. \quad \rightarrow \quad \rho''(r) + \frac{2}{r}\rho'(r) + \frac{1}{r_a^2}\rho(r) = 0.$$

In this approximation, the soliton density profile :

$$\rho_{\rm sol}(r) = \rho_{0\rm sol}\frac{\sin(\pi r/R_{\rm sol})}{\pi r/R_{\rm sol}},$$

$$R_{\rm sol} = \pi r_a, \quad \text{with } r_a^2 = \frac{3\lambda_4}{16\pi \mathcal{G}_N m^4}$$

r_a sets Jeans length !

I) Flat halo with r_a of the order of the system

Large soliton, Rsol = 0.5: interactions r_a **of the order of the system**

t=0 **t=150**

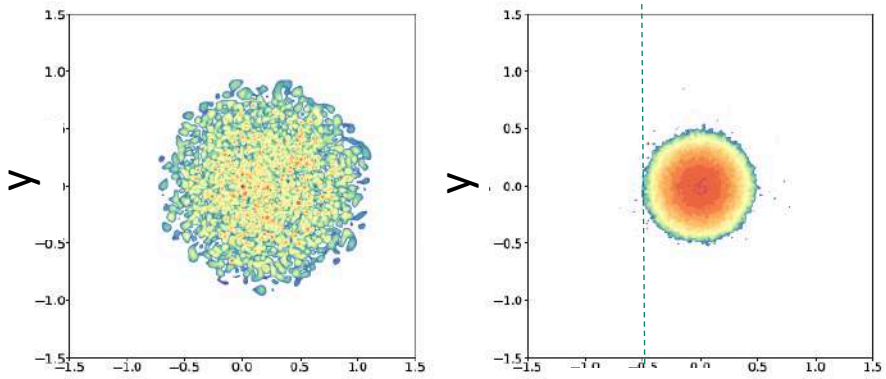

$$R_{sol} = \frac{\sqrt{\lambda\pi}}{2}, = 0.5$$

ρ_{max} , E_K, E_I, E_N

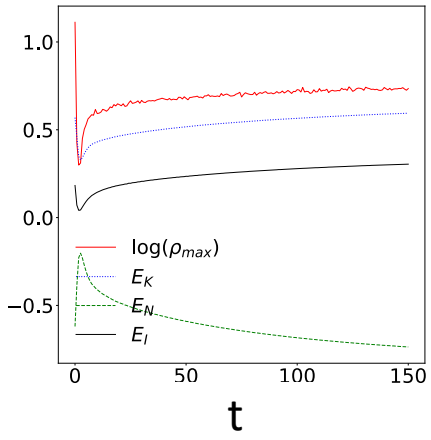

Potential at t=150

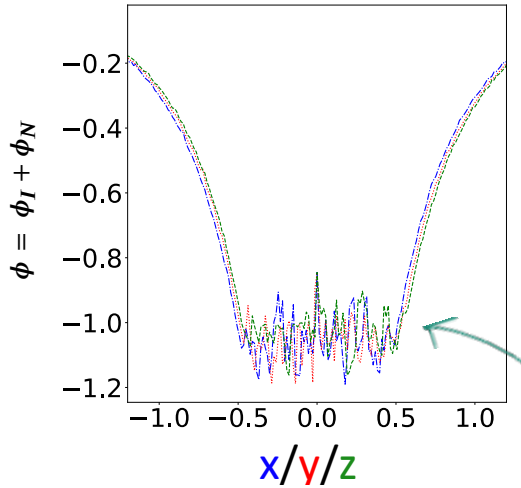

$$\Phi_N + \Phi_I = \alpha,$$

Soliton

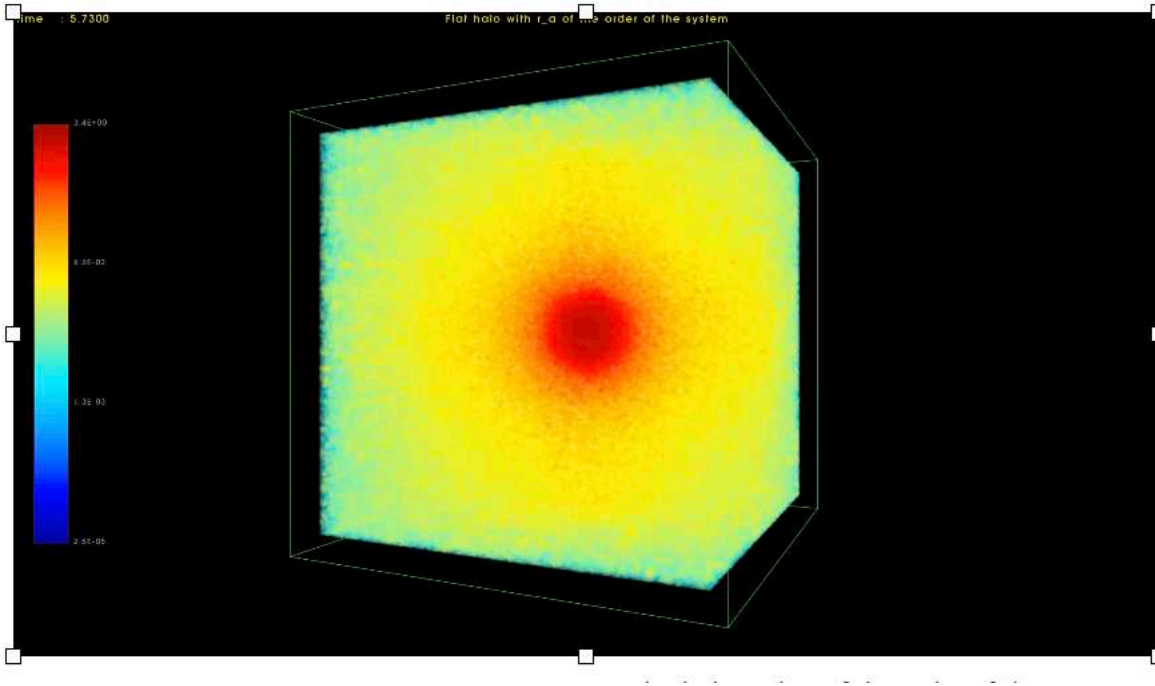

Flat halo with r_a of the order of the system

R.Galazo-García et al. (2024) acknowledgements to Jean Charles Lambert

Impact of baryons on self-interacting soliton cores ?

Thomas-Fermi regime → $\Phi_Q \ll \Phi_I$

Soliton TF limit

$$\Phi_N + \Phi_I = \alpha,$$

$$\rho_{\rm sol}(r) = \rho_{0\rm sol}\frac{\sin(\pi r/R_{\rm sol})}{\pi r/R_{\rm sol}},$$

$$R_{\rm sol} = \pi r_a, \quad \text{with} \quad r_a^2 = \frac{3\lambda_4}{16\pi \mathcal{G}_N m^4}$$

- Could we get an analytical solution for the inhomogeneous equation in the quartic self-interacting scenario?

$$\rho''(r) + \frac{2}{r}\rho'(r) + \frac{1}{r_a^2}\rho(r) + \rho_b(r) = 0.$$

Baryons: $$\rho_b(r) = \frac{\rho_{b0}}{(1 + r/rb)^\alpha}$$

Impact of baryons on self-interacting cores?

Baryons: $\alpha = 3$

$$\rho_b(r) = \frac{\rho_{b0}}{(1 + r/rb)^3}$$

Analytical Inhomegeneous solution

$$k = 1/r_a$$

$$\rho_2(r) = \frac{r_{b0}^3 \rho_{b0}}{2r(r + r_{b0})} \left[r_{b0} + (r + r_{b0}) \left(\mathrm{Ci}(k(r + r_{b0})) \cdot (2\cos(k(r + r_{b0})) - k r_{b0} \sin(k(r + r_{b0}))) \right.\right.$$

$$\left.\left. + (k r_{b0} \cos(k(r + r_{b0})) + 2\sin(k(r + r_{b0}))) \cdot \left(-\frac{\pi}{2} + \mathrm{Si}(k(r + r_{b0})) \right) \right) \right]$$

$$- \frac{r_{b0}^3 \rho_{b0}}{2r} \left[1 + \mathrm{Ci}(k r_{b0}) \cdot (2\cos(k r_{b0}) - k r_{b0} \sin(k r_{b0})) + (k r_{b0} \cos(k r_{b0}) + 2\sin(k r_{b0})) \cdot \left(-\frac{\pi}{2} + \mathrm{Si}(k r_{b0}) \right) \right] \cdot \cos(kr)$$

$$+ \frac{\rho_{s0}}{kr} \cdot \sin(kr)$$

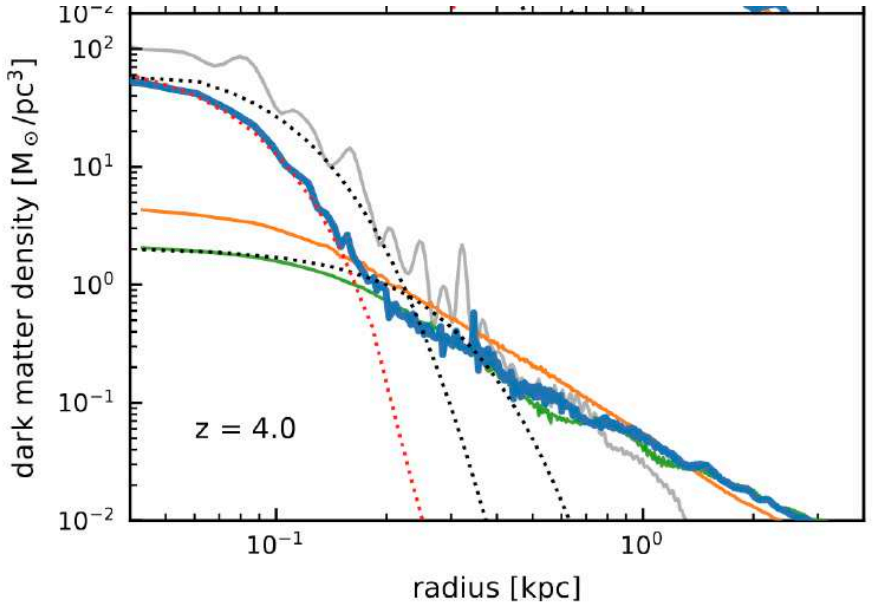

Jan Veltmaat, Bodo Schwabe, and Jens C. Niemeyer (2020)

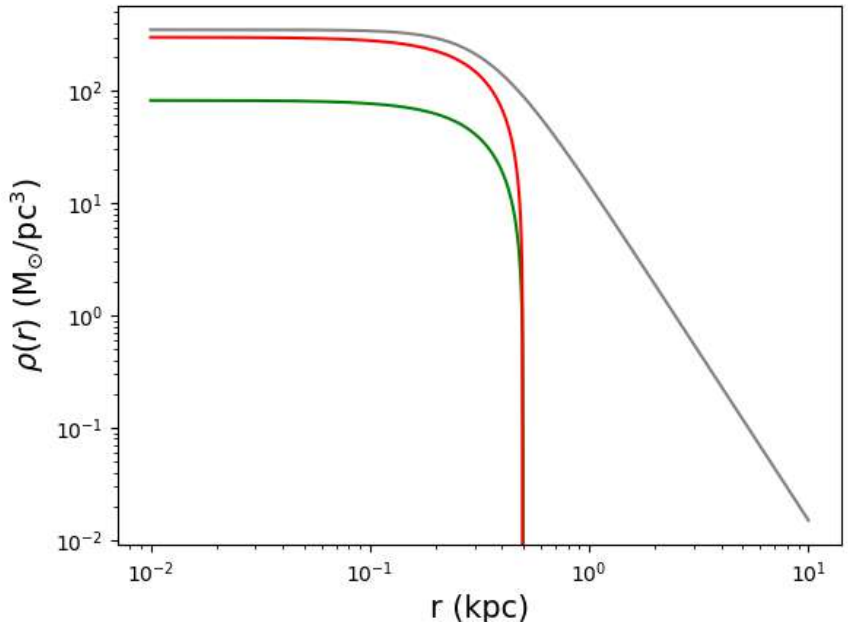

Impact of baryons on self-interacting cores?

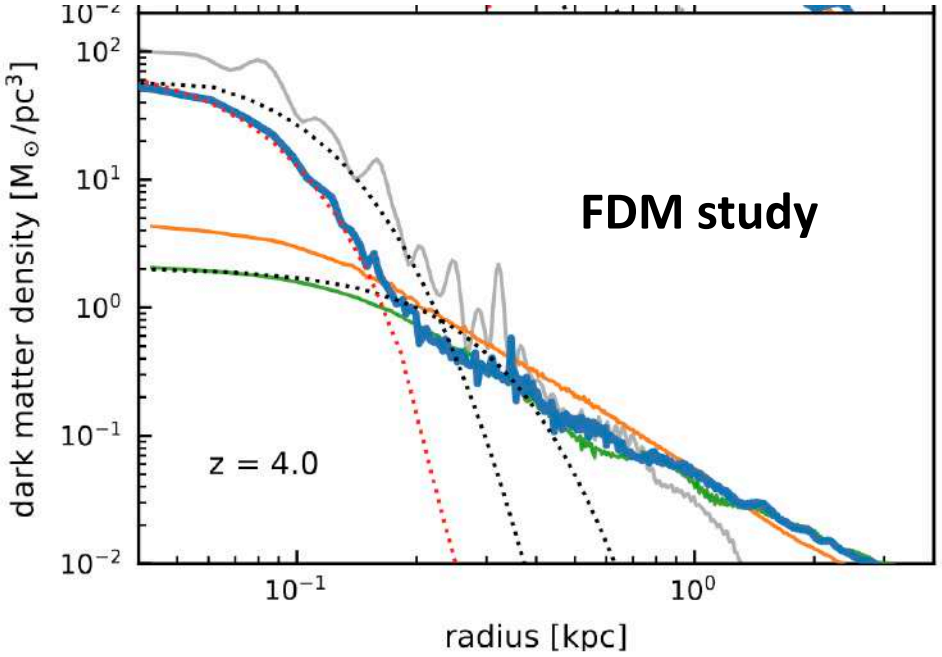

Jan Veltmaat, Bodo Schwabe, and Jens C. Niemeyer (2020)

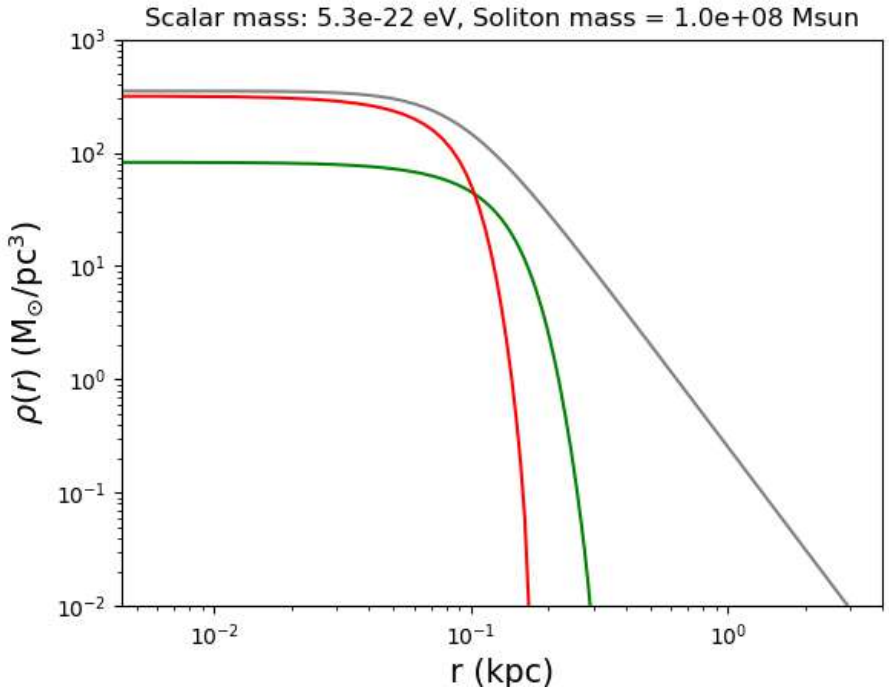

Numerical solution: Time-independent SP system

$$\psi = \psi_\star \tilde{\psi}, \quad t = t_\star \tilde{t}, \quad \vec{x} = L_\star \tilde{\vec{x}}, \quad \Phi = \frac{L_\star^2}{t_*^2}\tilde{\Phi},$$

$$\epsilon = \frac{t_\star}{m L_\star^2}. \qquad t_\star = \frac{1}{\sqrt{\mathcal{G}_N \rho_\star}}, \quad \rho = \rho_\star \tilde{\rho},$$

$$-\frac{\epsilon^2}{2}\left(\frac{d^2\tilde{\psi}}{d\tilde{r}^2} + \frac{2}{\tilde{r}}\frac{d\tilde{\psi}}{d\tilde{r}}\right) + \left(\tilde{\Phi}_N(\tilde{r}) + \tilde{\Phi}_I(\tilde{r})\right)\tilde{\psi}(\tilde{r}) = \tilde{\mu}\,\tilde{\psi}(\tilde{r})$$

$$\frac{d^2\tilde{\Phi}_N}{d\tilde{r}^2} + \frac{2}{\tilde{r}}\frac{d\tilde{\Phi}_N}{d\tilde{r}} = 4\pi\left|\tilde{\psi}(\tilde{r})\right|^2$$

Strong gravitational lensing signatures in galaxy clusters for self-interacting SFDM

- **DM structures (solitons)** leave a gravitational imprint on the multiple images of lensed sources.
- Multiple images provide a key test of different DM models → Independent of the baryonic content.

Self Interaction potential :

$$\Phi_I = \frac{3\lambda_4}{4m^3}|\psi|^2.$$

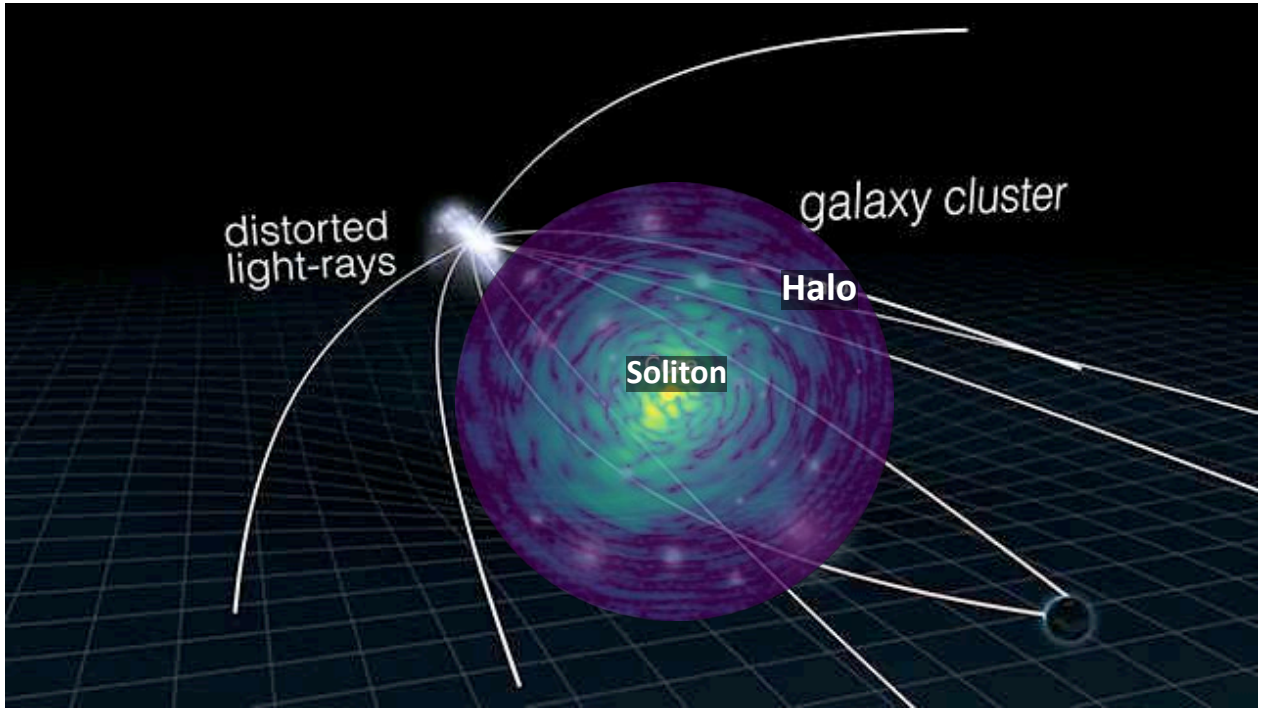

Scheme of strong gravitational lensing with SFDM
Credit 1: NASA, ESA & L. Calçada & Credit 2:

Total halo profile:

$$r < r_t: \quad \rho(r) = \rho_{0\mathrm{sol}} \frac{\sin(\pi r/R_{\mathrm{sol}})}{\pi r/R_{\mathrm{sol}}},$$

$$r_t < r < R: \quad \rho(r) = \frac{\rho_s}{\frac{r}{r_s}\left(1+\frac{r}{r_s}\right)^2}.$$

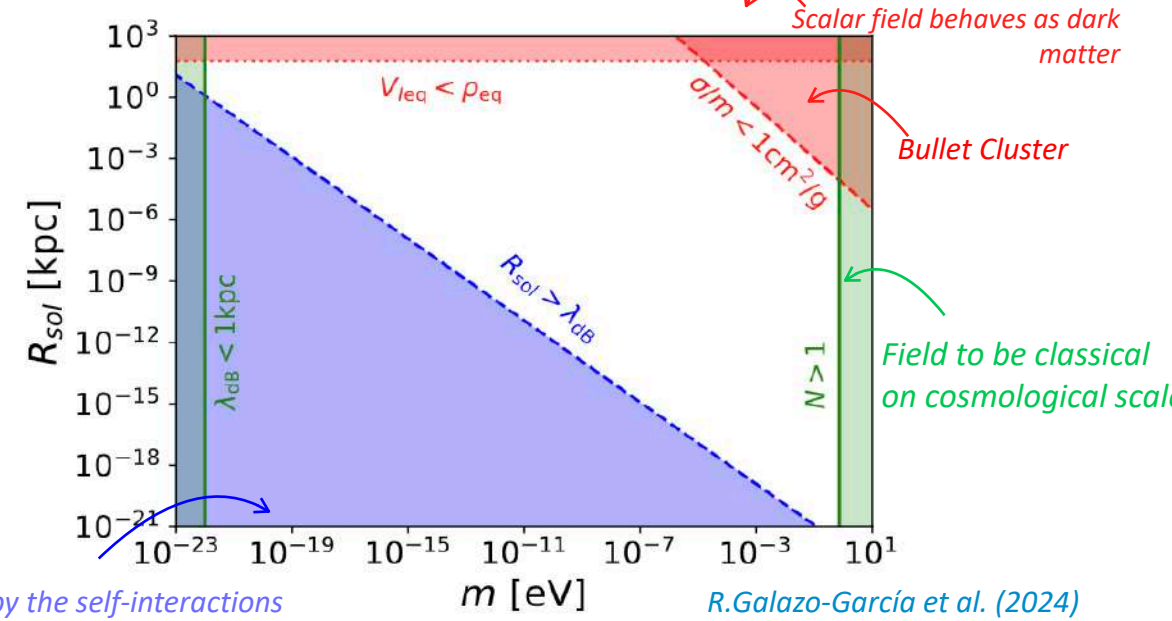

Soliton is governed by the self-interactions

R.Galazo-García et al. (2024)

General lensing equations

- We assume spherical symmetry and the thin approximation → size of the object is negligible compare to the angular distances.

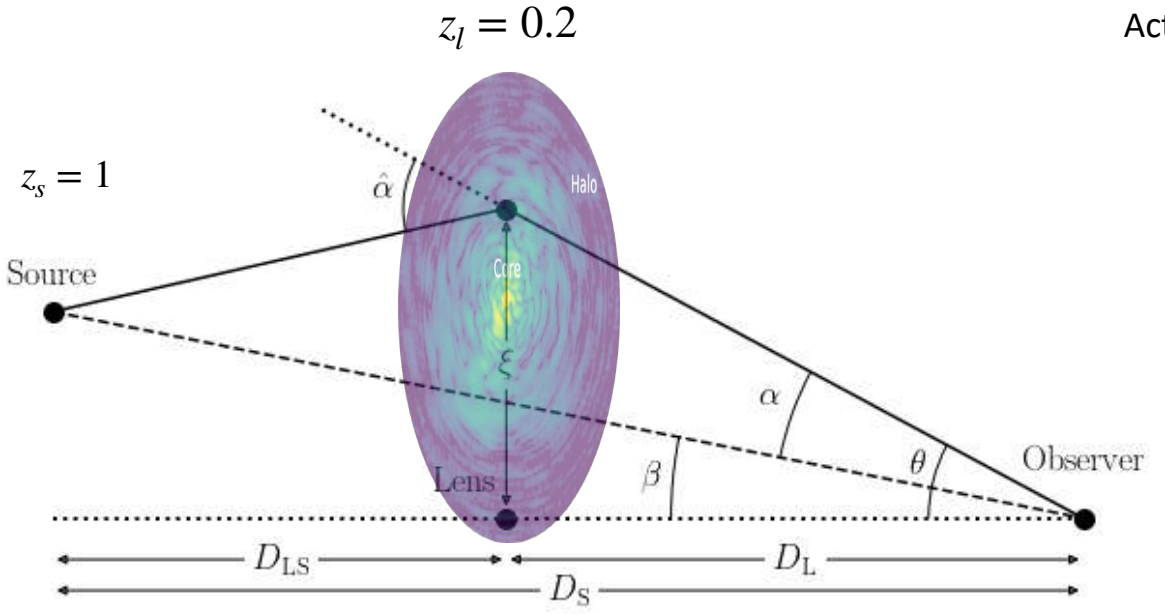

Actual unobservable angular position to the source

Deflection angle

$$\beta = \theta - \frac{D_{LS}}{D_S}\hat{\alpha}(\xi)$$

Observable apparent angular position to the image

$$\Sigma_{cr} \equiv \frac{c^2}{4\pi G}\frac{D_s}{D_l D_{ls}}$$

Deflection angle

$$\hat{\alpha}(\vec{\xi}) = \frac{4G}{c^2}\int \frac{(\vec{\xi} - \vec{\xi'})\Sigma(\vec{\xi'})}{|\vec{\xi} - \vec{\xi'}|} d^2\xi'$$

Surface mass density

$$\Sigma(\vec{\xi}) = \int \rho(\vec{\xi}, z) dz$$

Excess surface mass density

$$\Delta\Sigma(R) \equiv \bar{\Sigma}(< R) - \Sigma(R) = \Sigma_{cr}\gamma_+(R)$$

NFW - Deflection angle and surface mass density

- We build the NFW from the total mass of the system (→ r_{200}) and the concentration (→ r_s), and we get ρ_s .

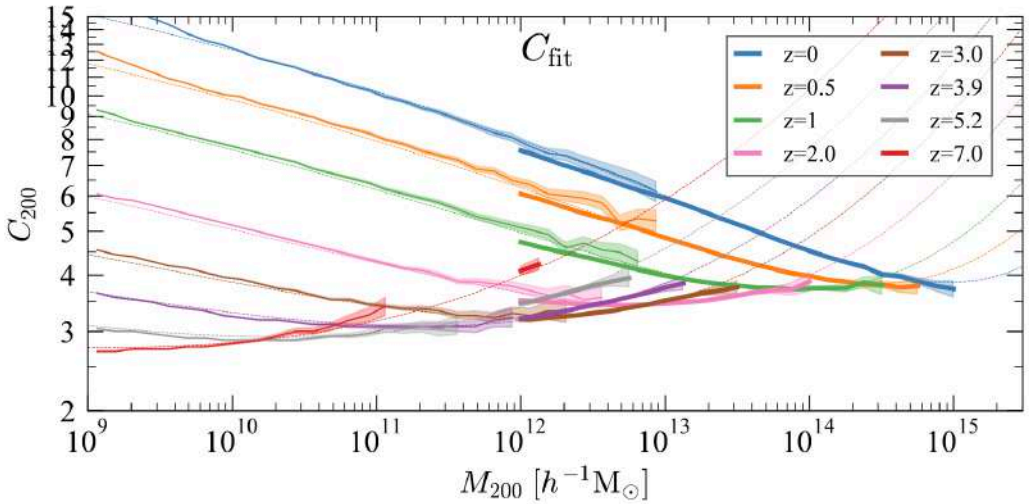

Mass-concentration relation of halos for the Uchuu simulation

Ishiyama et al. (2021)

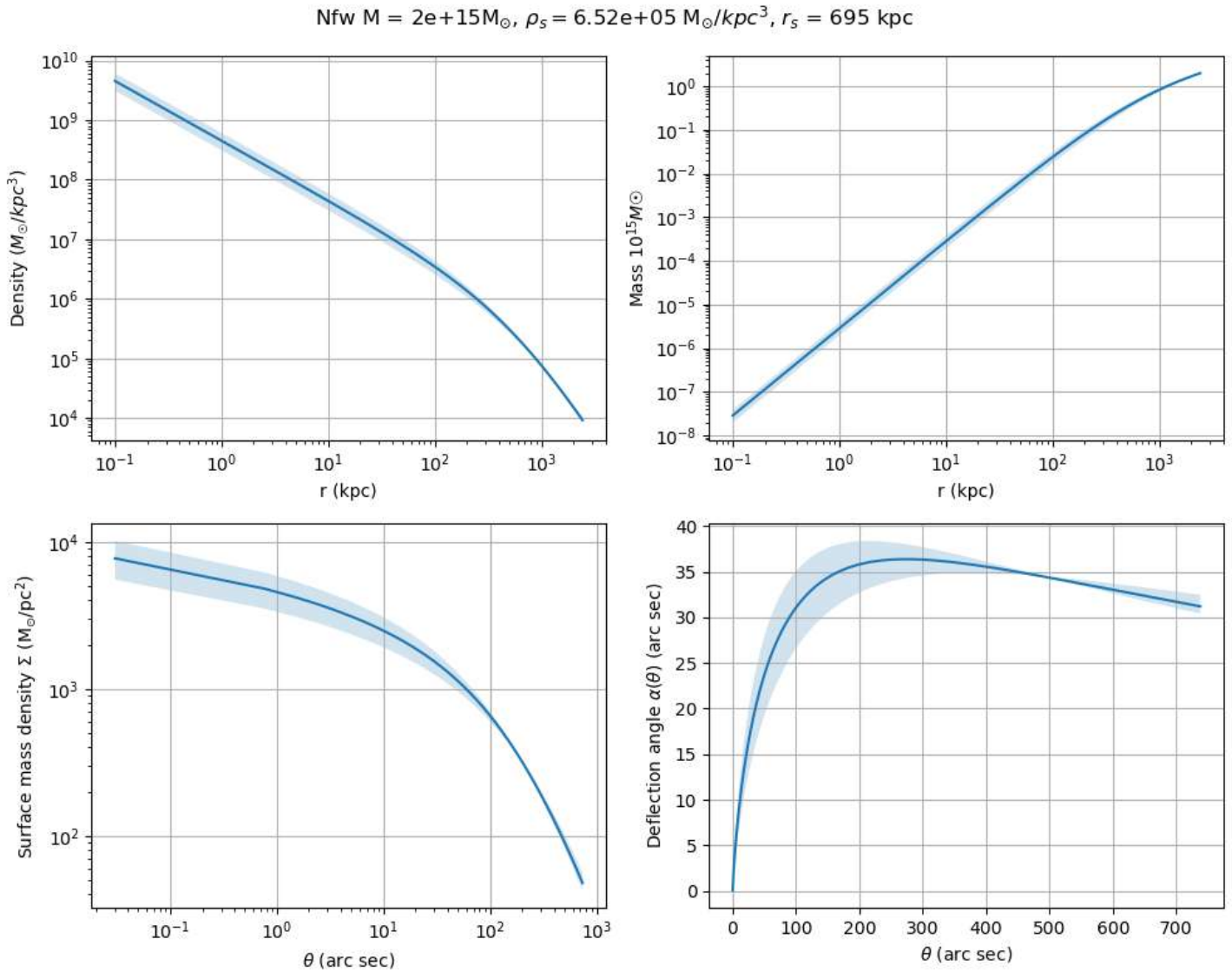

Total profile

- We choose the model to study $\rightarrow R_{sol} = \pi r_a$

$$r < r_t: \quad \rho(r) = \rho_{0\mathrm{sol}} \frac{\sin(\pi r/R_{\mathrm{sol}})}{\pi r/R_{\mathrm{sol}}},$$

$$r_t < r < R: \quad \rho(r) = \frac{\rho_s}{\frac{r}{r_s}\left(1+\frac{r}{r_s}\right)^2}.$$

- We calculate the value of r_t and ρ_{0sol} such that $M_{sol}(<r_t) = \alpha M_{NFW}(<r_t)$ and the total mass of the system is conserved.

- We have slight flexibility in the choice of α as long as we are in the Newtonian regime and the mass of the system varies minimally.

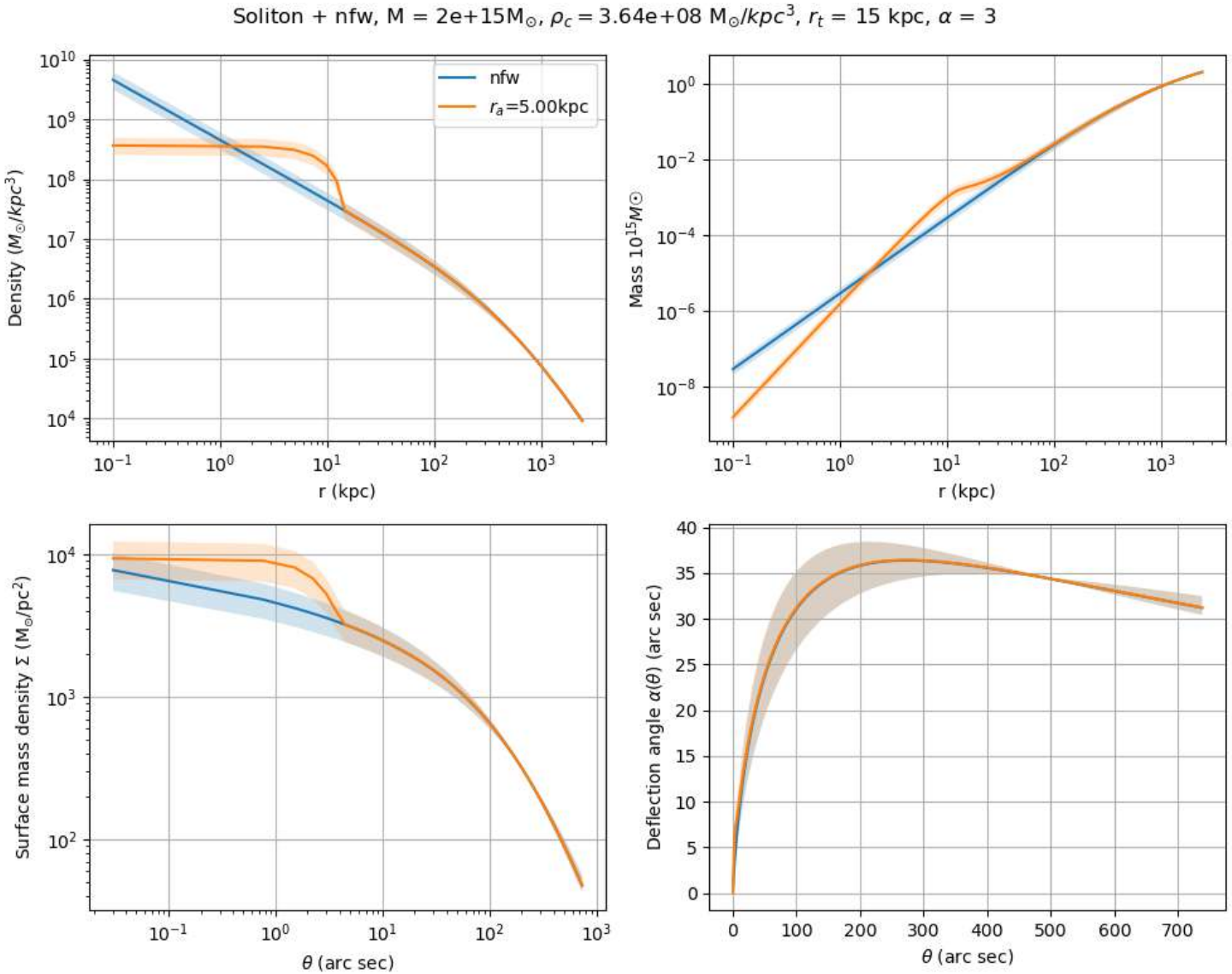

Study case: Halo $M \sim 10^{15} M_{\odot}$

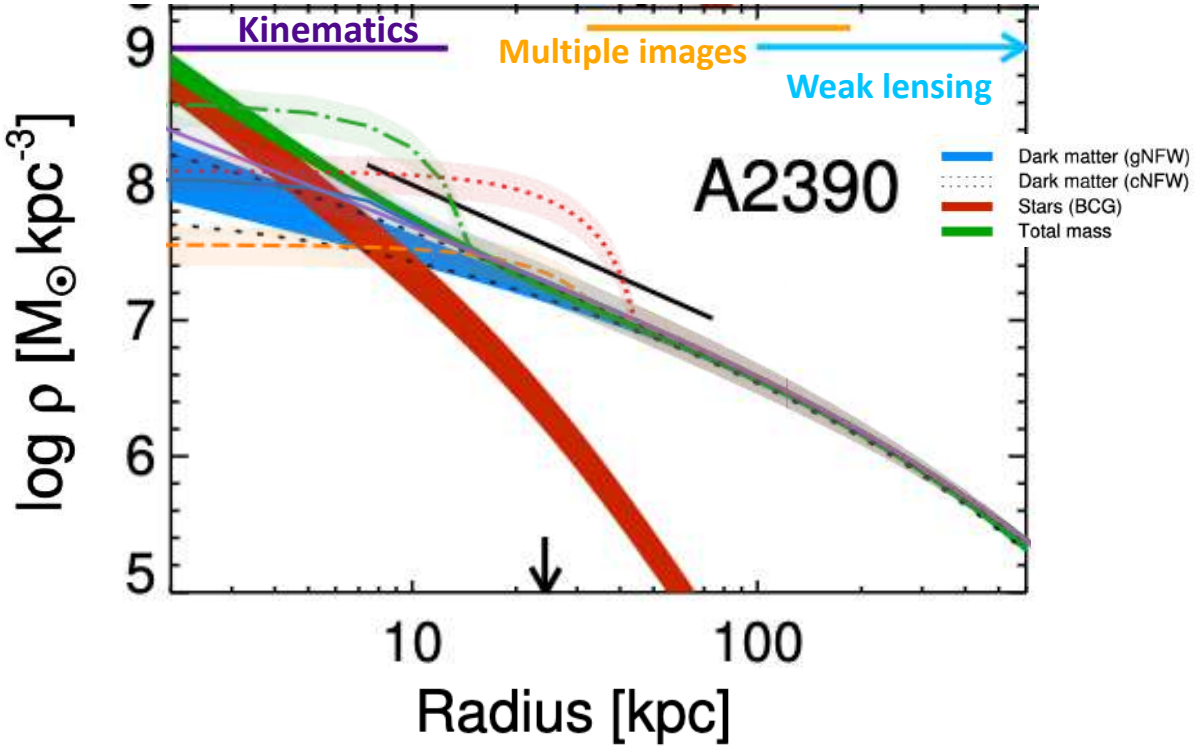

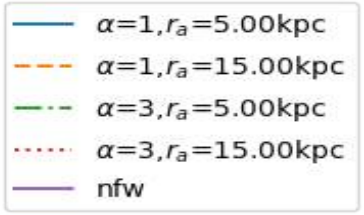

Halo $M = 2 \cdot 10^{15} M_{\odot}$						
α	r_a (kpc)	r_t (kpc)	ρ_c $(M_{\odot}/kpc^3)$	M_{sol} $(M_{\odot})$	$f_{sol}(\%)$	$\Delta M_h\%$
1	5	10.90	$1.02 \cdot 10^8$	$3.31 \cdot 10^{11}$	0.016	$8.28 \cdot 10^{-8}$
1	15	32.06	$3.26 \cdot 10^7$	$2.75 \cdot 10^{12}$	0.137	$6.15 \cdot 10^{-8}$
3	5	14.50	$3.64 \cdot 10^8$	$1.75 \cdot 10^{12}$	0.087	0.058
3	15	43.36	$1.14 \cdot 10^8$	$1.48 \cdot 10^{13}$	0.74	0.49

Comparison with Andrew B. Newman, Tommaso Treu, Richard S. Ellis, and David J. Sand, 2013

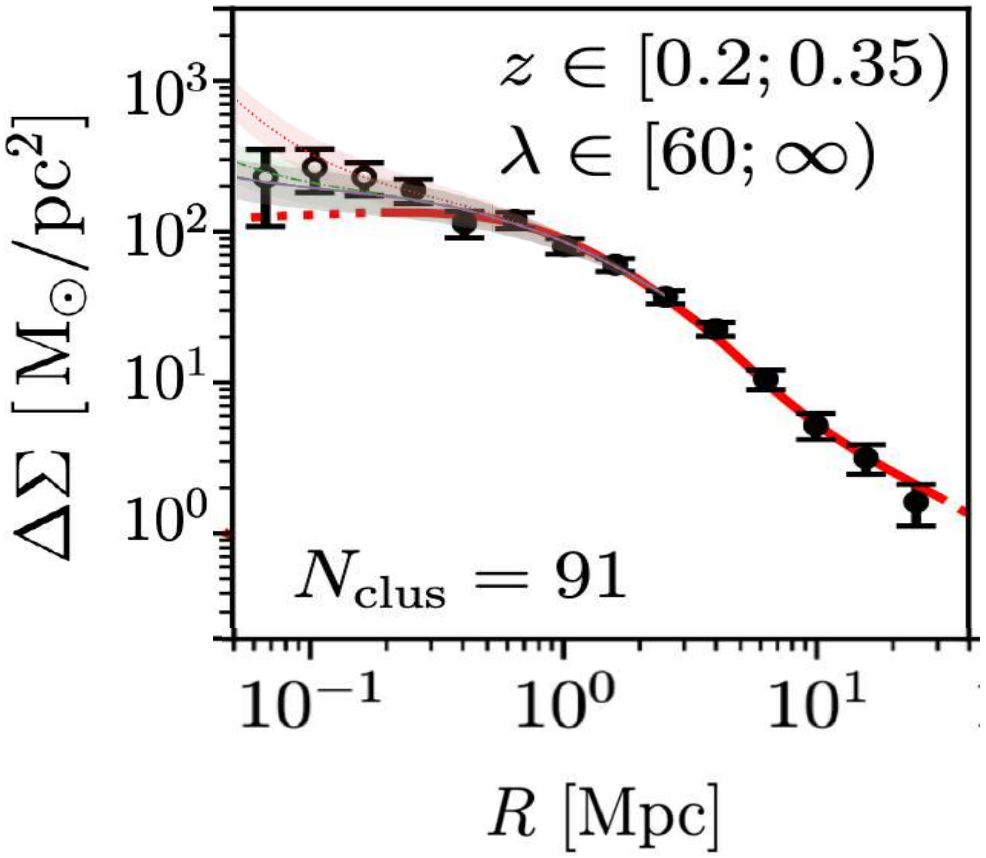

Comparison with Dark Energy Survey Year 1 Results: Weak Lensing Mass Calibration of redMaPPer Galaxy Clusters 2018

Study case: Halo $M \sim 10^{15} M_{\odot}$

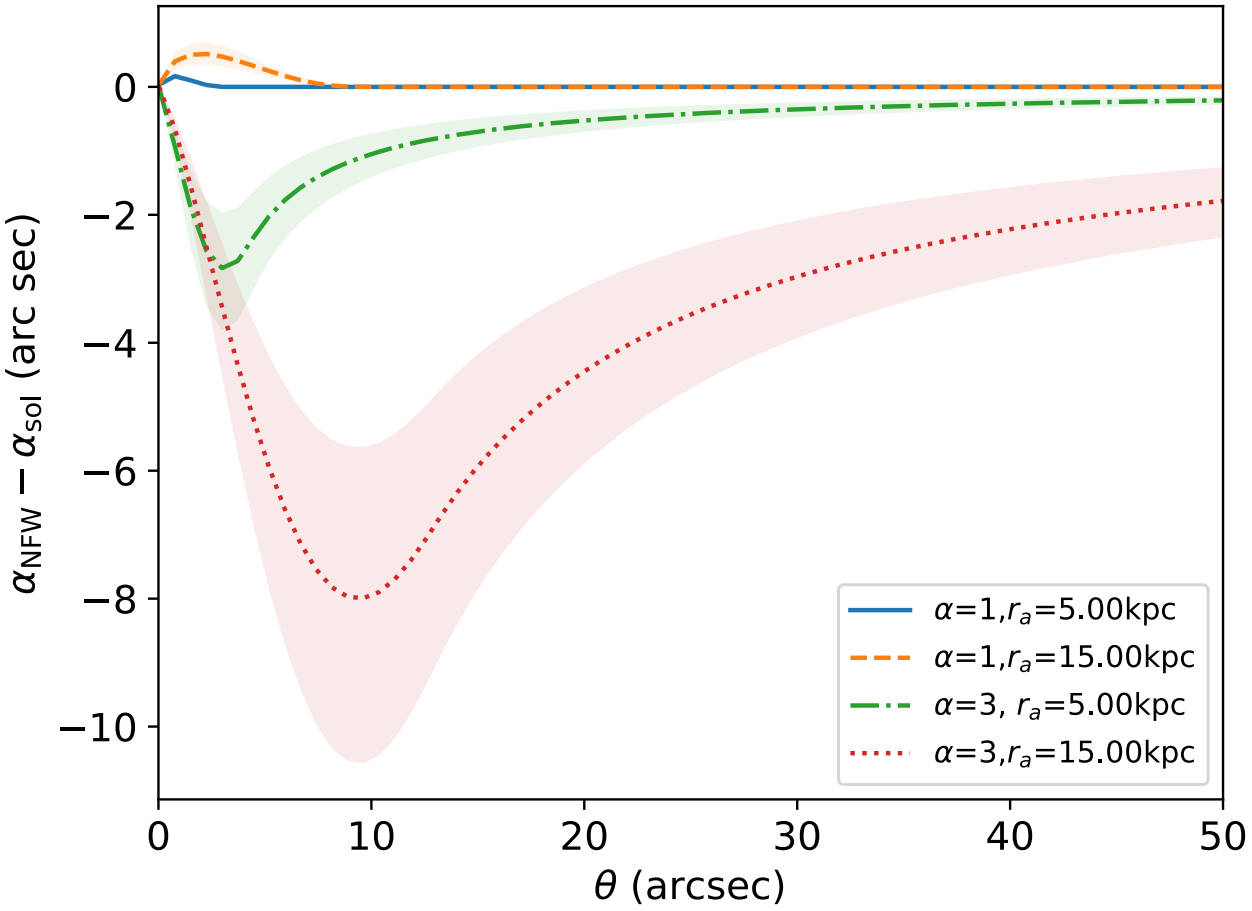

Difference of deflection angle NFW-Soliton

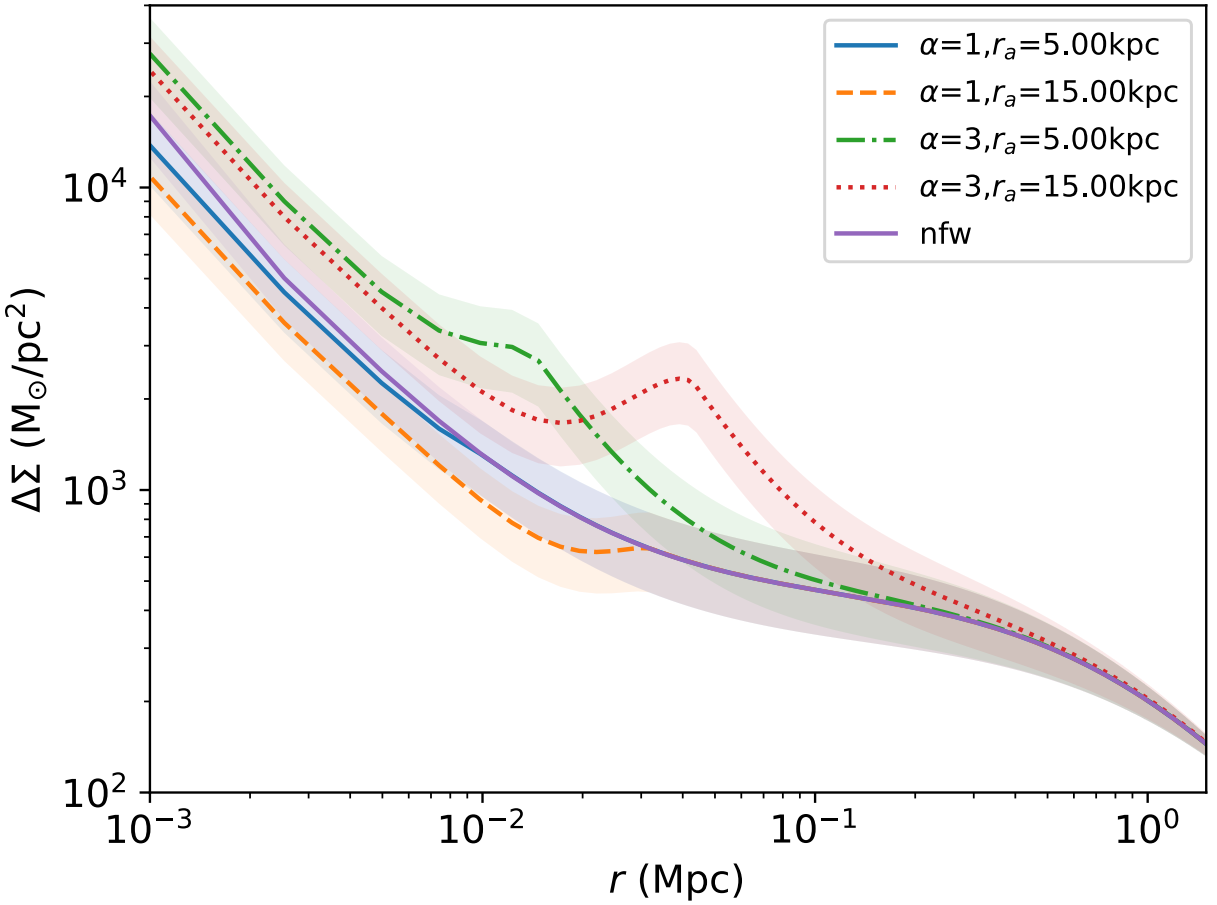

Excess surface mass density

Summary and outlook

- **SFDM as a strong alternative**: SFDM presents a promising alternative for describing dark matter.
- **Lensing patterns**: Differences in SI-SFDM density create distinct gravitational lensing signatures
- **Parameter constraints**: Preliminary results suggest we can constrain SI-SFDM parameters.
- **Soliton mass constraints**: We can accurately constrain the soliton mass in SI-SFDM → Core halo relation in this model.
- **Baryonic compression**
- **LENSTOOL implementation:** Calculating profiles using LENSTOOL enhances our SFDM analysis.

Constraining Scalar Field Dark Matter scenarios with Gravitational Lensing

Thank you for your attention

Raquel Galazo-García

D. Parameter space

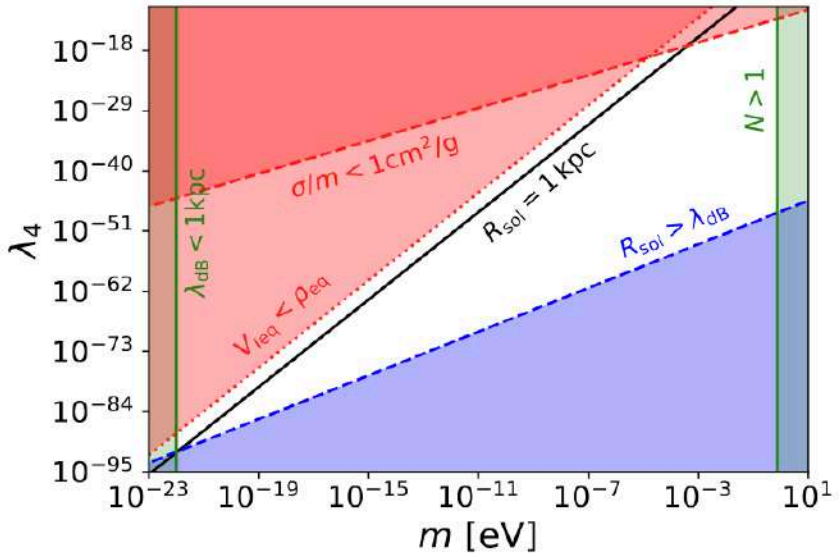

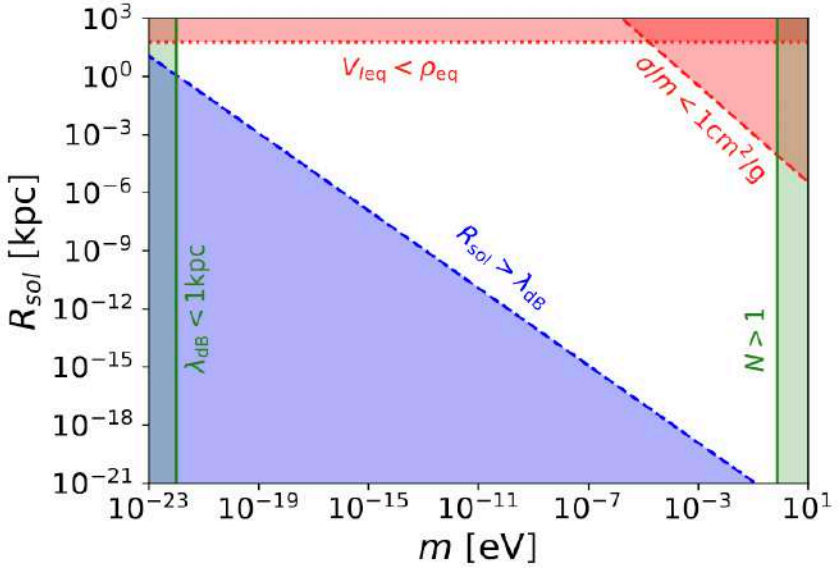

Difference NFW - Soliton deflection angle

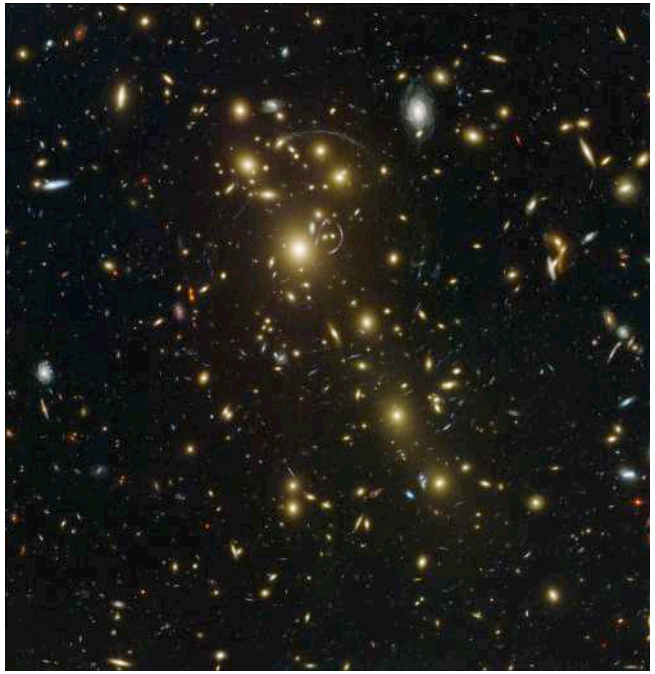

Abell 1709

Credit: NASA, ESA, and Johan Richard (Caltech, USA)

$r_a = 5\text{kpc} \rightarrow \rho_c \sim 3.72 \cdot 10^8 M_\odot/\text{kpc}^3$

$r_a = 15\text{kpc} \rightarrow \rho_c \sim 1.17 \cdot 10^8 M_\odot/\text{kpc}^3$

NFW : $r_s = 800$ kpc, $\rho_s \sim 5.77 \cdot 10^5 M_\odot/\text{kpc}^3$

- $M = 2 \cdot 10^{15} M_\odot$, $\alpha = 3$

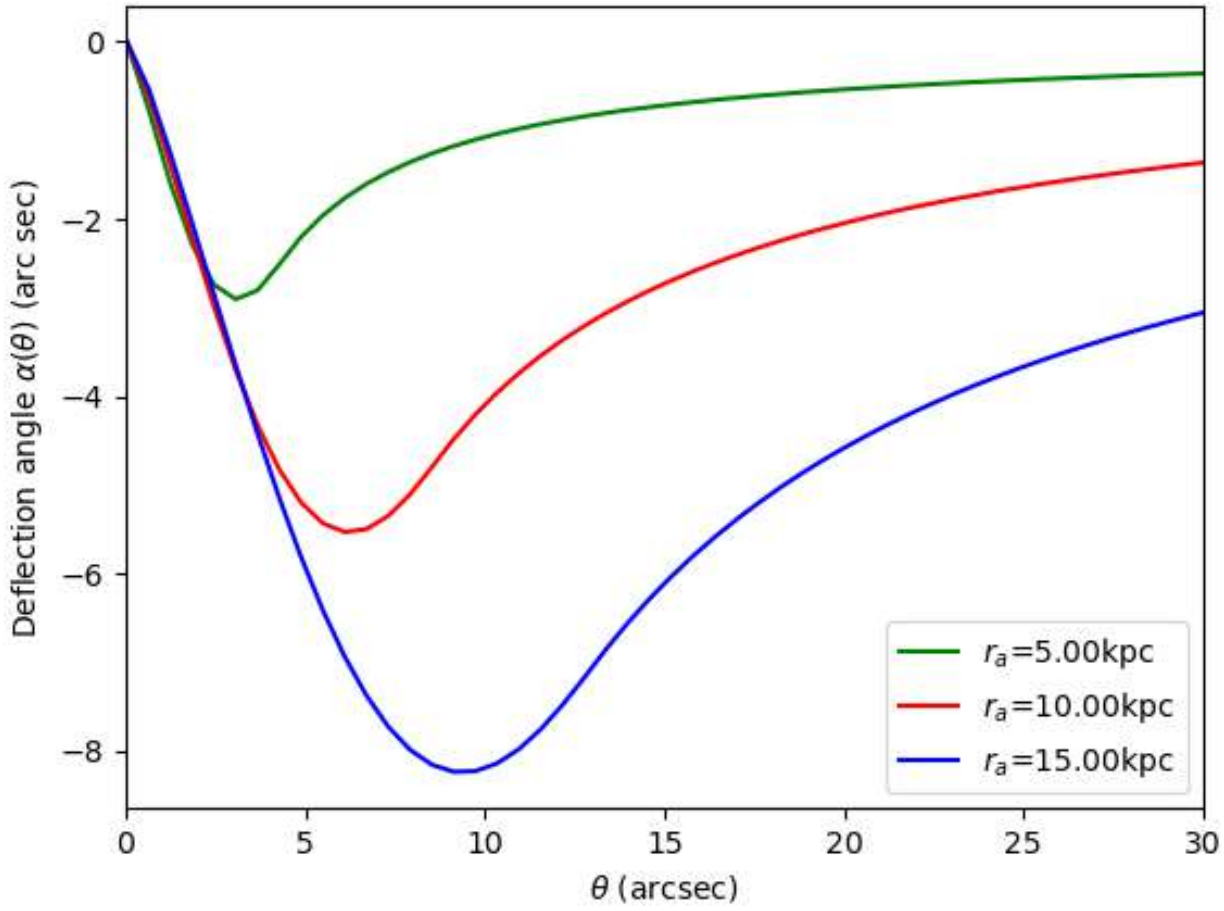

Difference of deflection angle NFW-Soliton

Halo $M = 2 \cdot 10^{15} M_\odot$						
α	r_a (kpc)	r_t (kpc)	ρ_c $(M_\odot/kpc^3)$	M_{sol} $(M_\odot)$	$f_{sol}(\%)$	$\Delta M_h\%$
1	5	10.90	$1.02 \cdot 10^8$	$3.31 \cdot 10^{11}$	0.016	$8.28 \cdot 10^{-8}$
1	15	32.06	$3.26 \cdot 10^7$	$2.75 \cdot 10^{12}$	0.137	$6.15 \cdot 10^{-8}$
3	5	14.50	$3.64 \cdot 10^8$	$1.75 \cdot 10^{12}$	0.087	0.058
3	15	43.36	$1.14 \cdot 10^8$	$1.48 \cdot 10^{13}$	0.74	0.49

TABLE IX. Soliton profile configurations for $M = 2 \cdot 10^{15} M_\odot$

Halo $M = 2 \cdot 10^{14} M_\odot$						
α	r_a (kpc)	r_t (kpc)	ρ_c $(M_\odot/kpc^3)$	M_{sol} $(M_\odot)$	$f_{sol}(\%)$	$\Delta M_h\%$
1	5	11.21	$6.20 \cdot 10^7$	$2.12 \cdot 10^{11}$	0.11	$8.95 \cdot 10^{-8}$
1	15	33.94	$1.8 \cdot 10^7$	$1.74 \cdot 10^{12}$	0.87	$1.87 \cdot 10^{-9}$
3	5	14.50	$2.18 \cdot 10^8$	$1.05 \cdot 10^{12}$	0.52	0.34
3	15	43.36	$6.30 \cdot 10^7$	$8.15 \cdot 10^{12}$	4.08	2.71

TABLE X. Soliton profile configurations for $M = 2 \cdot 10^{14} M_\odot$

Halo $M = 2 \cdot 10^{13} M_\odot$						
α	r_a (kpc)	r_t (kpc)	ρ_c $(M_\odot/kpc^3)$	M_{sol} $(M_\odot)$	$f_{sol}(\%)$	$\Delta M_h\%$
1	5	11.50	$3.76 \cdot 10^7$	$1.34 \cdot 10^{11}$	0.64	$8.54 \cdot 10^{-8}$
1	15	35.83	$9.42 \cdot 10^6$	$9.70 \cdot 10^{11}$	4.85	$6.40 \cdot 10^{-8}$
3	5	14.50	$1.28 \cdot 10^8$	$6.18 \cdot 10^{11}$	3.09	2.06
3	15	44.30	$3.10 \cdot 10^7$	$4.06 \cdot 10^{12}$	20.30	13.54

TABLE XI. Soliton profile configurations for $M = 2 \cdot 10^{13} M_\odot$

$M_h(M_\odot)$	Fit $\rho_s(M_\odot/kpc^3)$	Fit r_s (kpc)
$2 \cdot 10^{13}$	$2.90 \cdot 10^5 \pm 0.035$	183.34 ± 2.83
$2 \cdot 10^{14}$	$2.40 \cdot 10^5 \pm 1.03$	429.65 ± 6.46
$2 \cdot 10^{15}$	$3.97 \cdot 10^5 \pm 1.03$	784.85 ± 9.86

TABLE V. NFW with $\alpha = 1$, $\beta = 3$, $\gamma = 1.5$

$$\rho(r) = \frac{\rho_s}{\left(\frac{r}{r_s}\right)^\gamma \left(1 + \left(\frac{r}{r_s}\right)^\alpha\right)^{(\beta-\gamma)/\alpha}}$$

TABLE 8
NFW Parameters Derived from X-Ray and Lensing Analyses

Cluster	X-Ray			Lensing (Strong + Weak)			
	r_s (kpc)	c_{200}	Source	r_s (kpc)	c_{200}	$\log M_{200}/\mathrm{M}_\odot$	r_{200} (kpc)
MS2137	180^{+20}_{-20}	$8.19^{+0.54}_{-0.56}$	S07	119^{+49}_{-32}	$11.03^{+2.81}_{-2.39}$	$14.56^{+0.13}_{-0.11}$	1318^{+140}_{-107}
A963	390^{+120}_{-80}	$4.73^{+0.84}_{-0.77}$	S07	197^{+48}_{-52}	$7.21^{+1.59}_{-0.94}$	$14.61^{+0.11}_{-0.15}$	1430^{+127}_{-151}
A383	470^{+130}_{-100}	$3.8^{0.7}_{-0.5}$	A08	260^{+59}_{-45}	$6.51^{+0.92}_{-0.81}$	$14.82^{+0.09}_{-0.08}$	1691^{+128}_{-102}
A383 (prolate)	...	...	...	372^{+63}_{-51}	$4.49^{+0.50}_{-0.48}$	14.80 ± 0.08	1665^{+107}_{-95}
A611	320^{+200}_{-100}	$5.39^{+1.60}_{-1.51}$	S07	317^{+57}_{-47}	$5.56^{+0.65}_{-0.60}$	14.92 ± 0.07	1760^{+97}_{-89}
A2537	370^{+310}_{-150}	$4.86^{+2.06}_{-1.62}$	S07	442^{+46}_{-44}	$4.63^{+0.35}_{-0.30}$	15.12 ± 0.04	2050^{+65}_{-69}
A2667	700^{+479}_{-207}	$3.02^{+0.74}_{-0.85}$	A03	725^{+118}_{-109}	$2.99^{+0.32}_{-0.27}$	15.16 ± 0.08	2164^{+137}_{-129}
A2390	757^{+1593}_{-393}	$3.20^{+1.59}_{-1.57}$	A03	763^{+119}_{-107}	$3.24^{+0.35}_{-0.31}$	$15.34^{+0.06}_{-0.07}$	2470^{+112}_{-123}

Note. — All X-ray fits are to the total gravitating mass and have been standardized to the same cosmology. Sources: S07 = Schmidt & Allen (2007), A08 = Allen et al. (2008), A03 = Allen et al. (2003). The A383 (prolate) row shows a fit to lensing and X-ray data using triaxial isodensity surfaces (Equation 14, and see N11); we report sphericalized NFW parameters in this case.

10**14

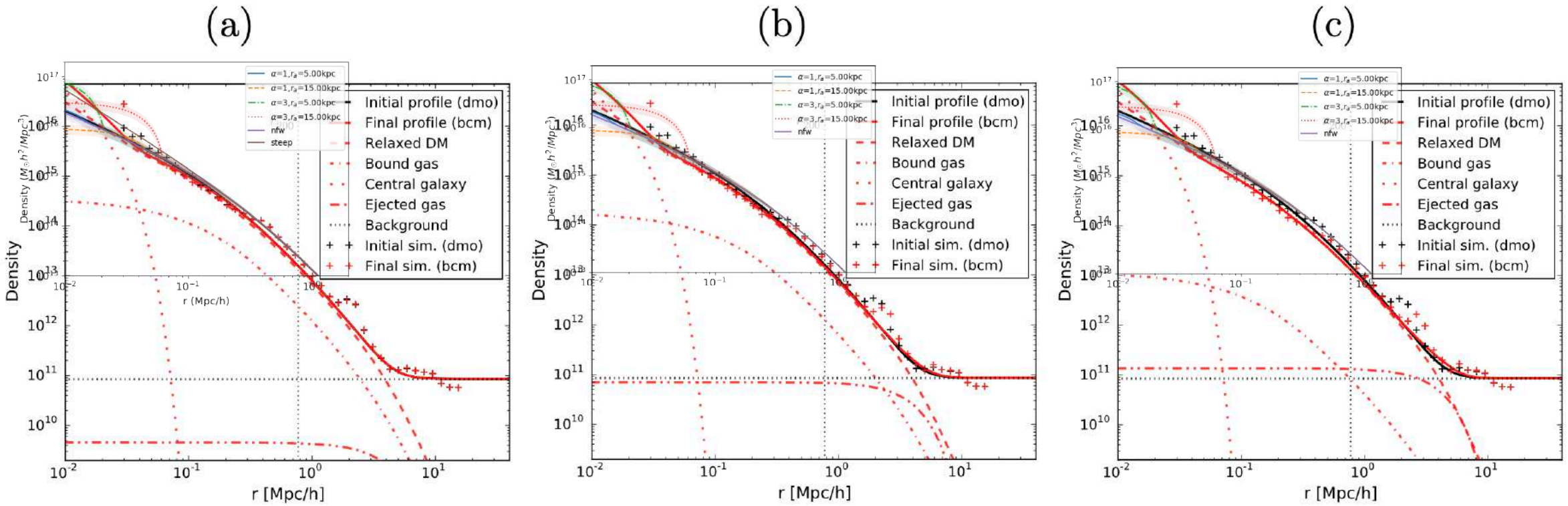
(a)
(b)
(c)
Density
r [Mpc/h]
r (Mpc/h)
α=1,r_a=5.00kpc
α=1,r_a=15.00kpc
α=3,r_a=5.00kpc
α=3,r_a=15.00kpc
nfw
steep
Initial profile (dmo)
Final profile (bcm)
Relaxed DM
Bound gas
Central galaxy
Ejected gas
Background
Initial sim. (dmo)
Final sim. (bcm)

Soliton - Deflection angle and surface mass density

$\alpha = 3,\ r_a = 5\ \text{kpc},\ r_t = 14\ \text{kpc}$

- $M = 2 \cdot 10^{14} M_\odot\,, \alpha = 3$

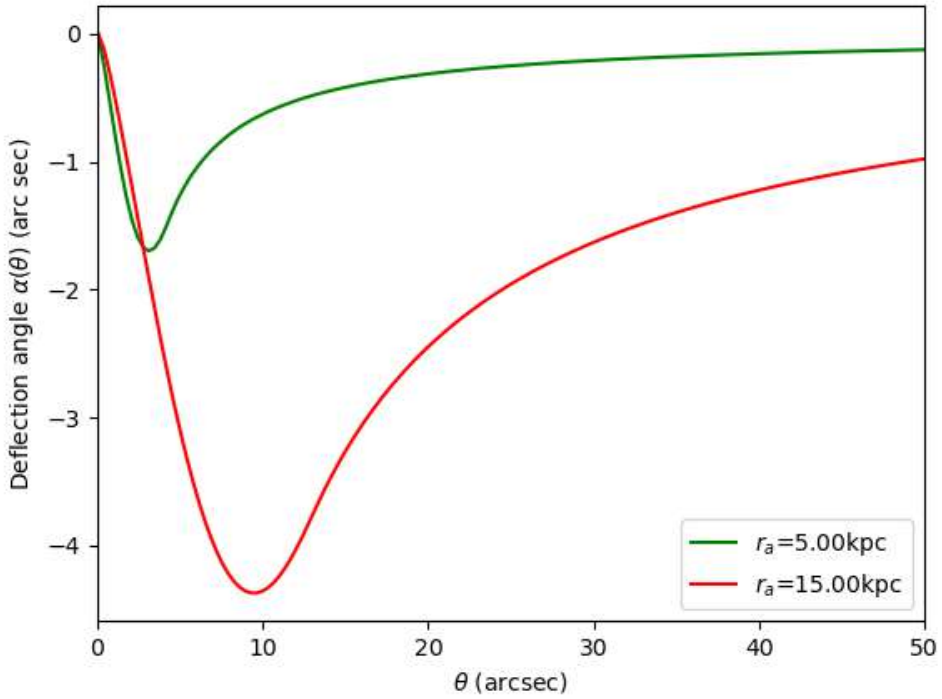

Difference of deflection angle NFW-Soliton

$$r_a = 5\text{kpc} \rightarrow \rho_c \sim 2.18 \cdot 10^8 M_\odot/\text{kpc}^3$$

$$r_a = 15\text{kpc} \rightarrow \rho_c \sim 6.30 \cdot 10^7 M_\odot/\text{kpc}^3$$

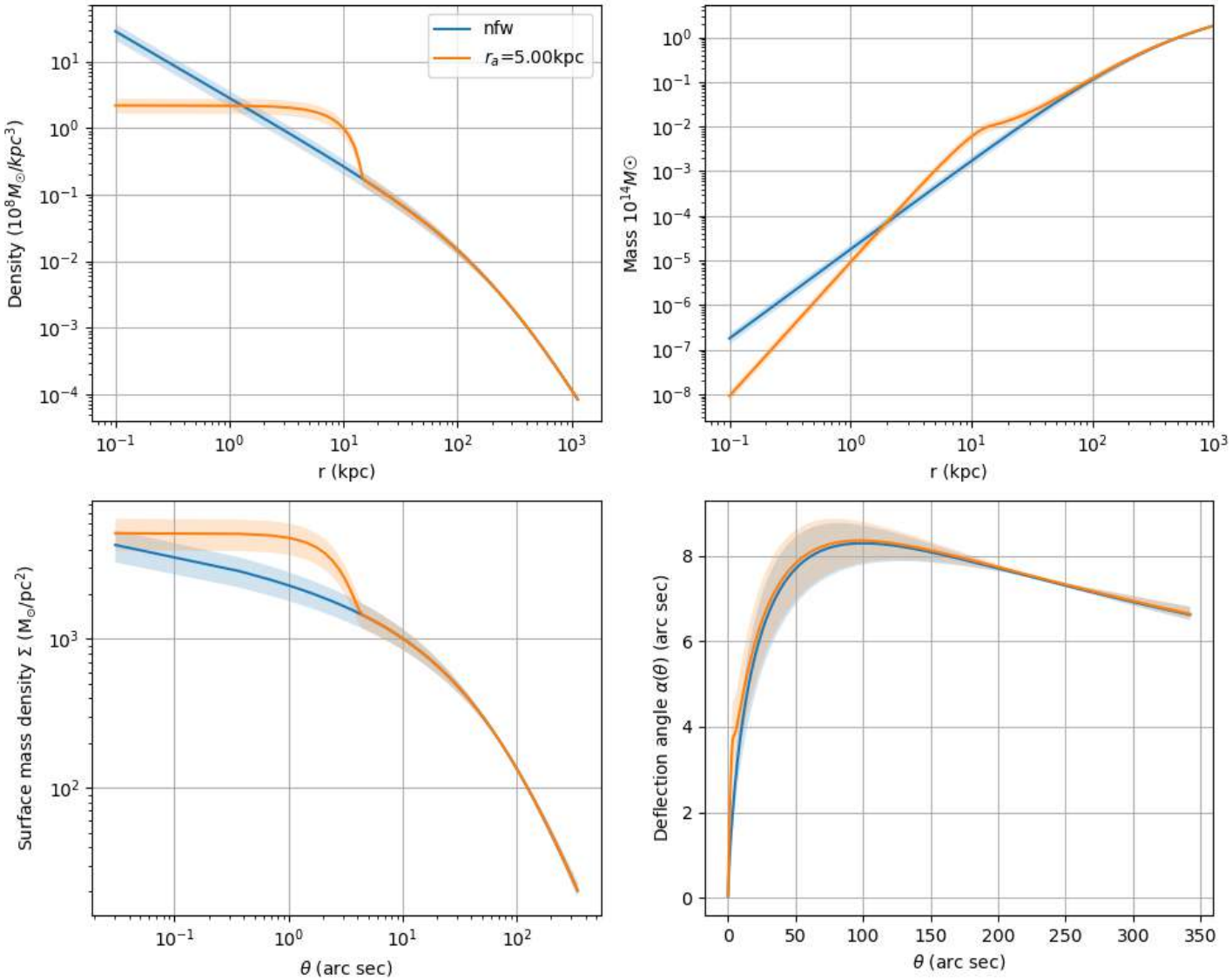

II) Flat halo with r_a much smaller than system

Small soliton, Rsol = 0.1: interactions r_a **much smaller than the system**

Density slice *2D (x,y)* at $z=r_{max,}$ (ρ_{max})

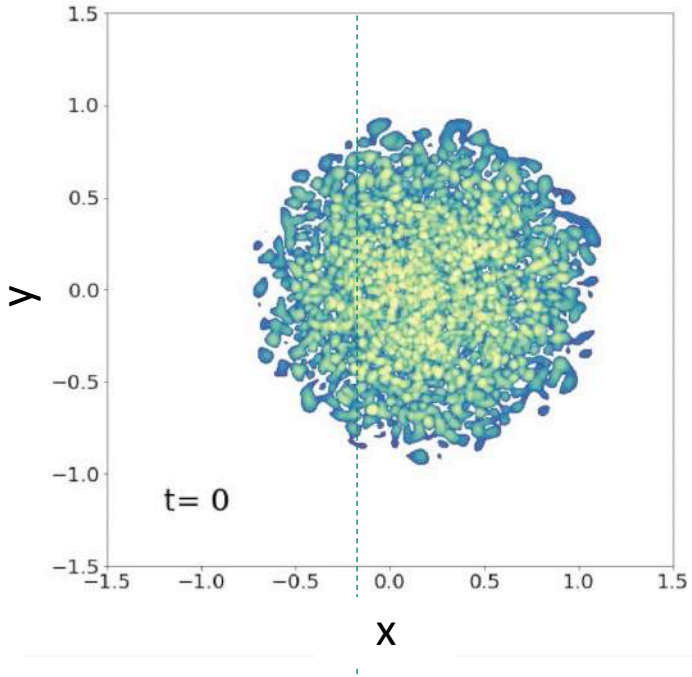

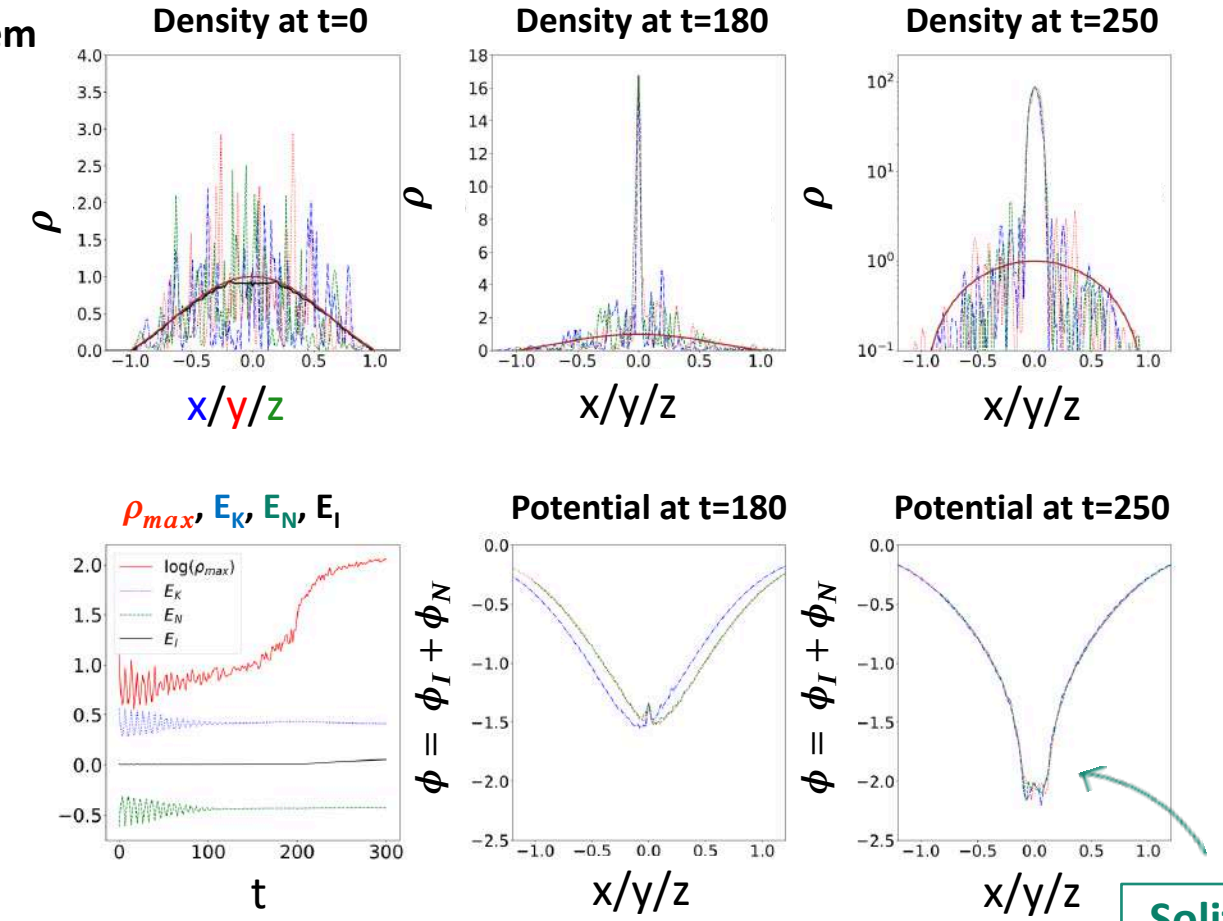

- By t ~ 100, the halo relaxes to a quasi-stationary state.
- At t ~180, FDM peak.
- At t ~ 200, self-interacting soliton forms, $R_{sol} = 0.1$.

R.Galazo-García, P.Brax and P.Valageas (2024)

Transition from a FDM phase to a self-interacting phase.

Non-polynomial self-interacting

$$i\epsilon\frac{\partial\tilde{\psi}}{\partial\tilde{t}} = -\frac{\epsilon^2}{2}\tilde{\nabla}^2\tilde{\psi} + (\tilde{\Phi}_N + \tilde{\Phi}_I)\tilde{\psi},$$

$$\tilde{\nabla}^2\tilde{\Phi}_N = 4\pi\tilde{\rho}, \quad \text{with} \quad \tilde{\rho} = |\tilde{\psi}|^2,$$

$$\tilde{\Phi}_I(\tilde{\rho}) = \begin{cases} \lambda\tilde{\rho} & \text{if} \quad \tilde{\rho} < \tilde{\rho}_c \\ \lambda\tilde{\rho}_c & \text{if} \quad \tilde{\rho} > \tilde{\rho}_c \end{cases}$$

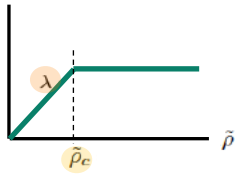

Low density regime:

$$\text{TF regime}: \quad \Phi_N + \Phi_I = \mu.$$

High density regime:

$$\text{FDM regime}: \quad \Phi_Q + \Phi_N = \mu - \lambda\rho_c,$$

Transition from a self-interacting phase to a FDM phase !

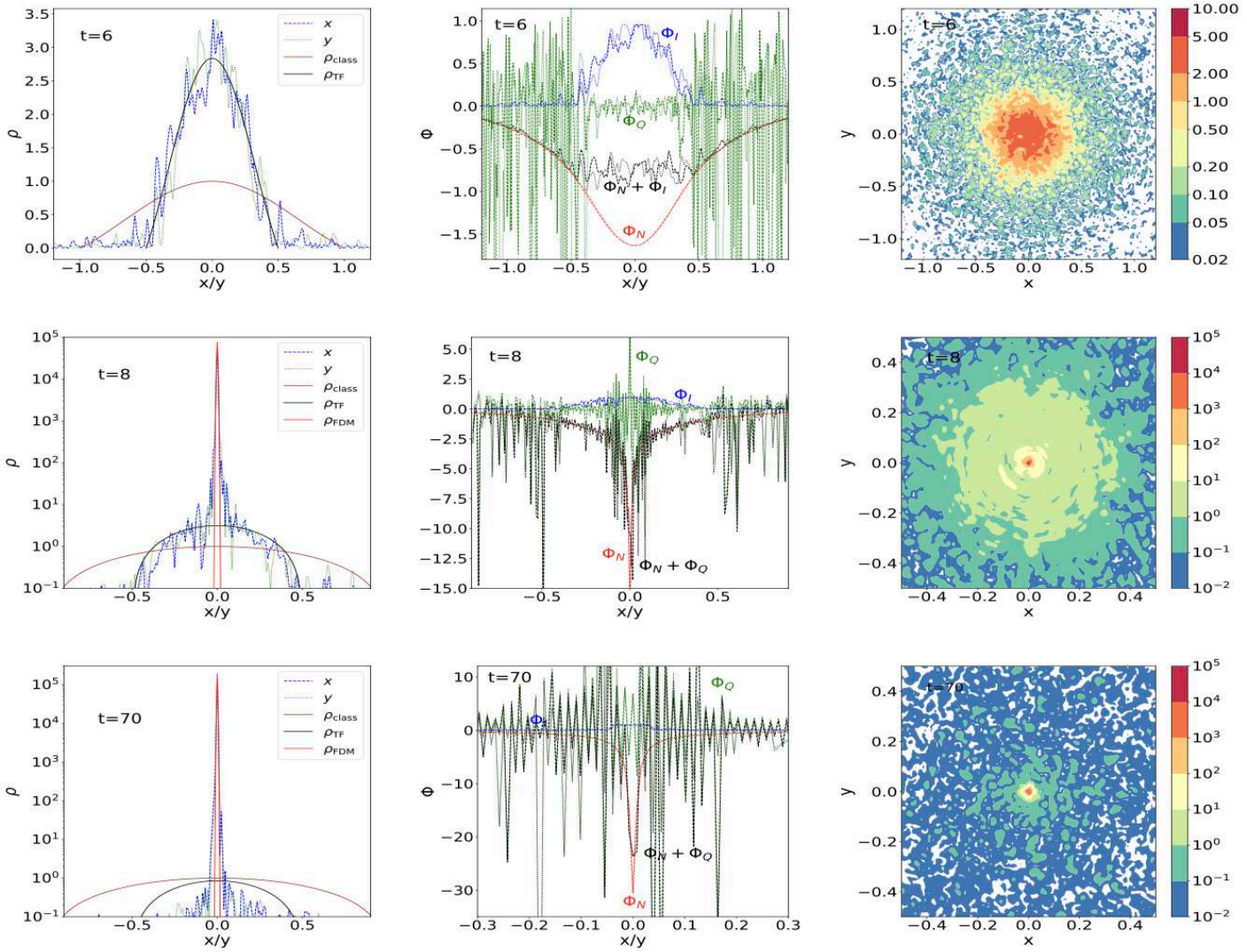

FIG. 4. Evolution of a halo with $R_{\rm TF} = 0.5$ and $\rho_c = 3$.

Upcoming preprint, check the arXiv these weeks!! R.Galazo-García, P.Brax and P.Valageas

Gaussian ansatz to describe the transition

$$\rho(r) = \rho_0\, e^{-(r/R)^2}, \quad \psi = \sqrt{\rho}, \quad \text{with} \quad \rho_0 = \frac{M}{\pi^{3/2} R^3}.$$

Energy functional

$$E_{\rm tot} = E_K + E_N + E_I = \int d\vec{x} \left(\frac{\epsilon^2}{2} |\nabla\psi|^2 + \frac{1}{2}\rho\Phi_N + \mathcal{V}_I \right)$$

Self-interacting energy:

$$\rho_0 < \rho_c: \quad E_I = \frac{\lambda}{4\sqrt{2}} M \rho_0,$$

$$\rho_0 > \rho_c: \; E_I = \frac{\lambda M \rho_0}{4\sqrt{2}} \left[\mathrm{Erfc}\left(\sqrt{2 \ln \frac{\rho_0}{\rho_c}} \right) + 4\sqrt{2} \frac{\rho_c}{\rho_0} \times \mathrm{Erf}\left(\sqrt{\ln \frac{\rho_0}{\rho_c}} \right) - \frac{2\sqrt{2}}{3\sqrt{\pi}} \frac{\rho_c^2}{\rho_0^2} \sqrt{\ln \frac{\rho_0}{\rho_c}} \left(9 + 4 \ln \frac{\rho_0}{\rho_c} \right) \right],$$

Gravitational energy

$$E_N = -\frac{1}{\sqrt{2}} M^{5/3} \rho_0^{1/3}.$$

Kinetic energy

$$E_K = \epsilon^2 \frac{3\pi}{4} M^{1/3} \rho_0^{2/3},$$

Soliton condition

$$\frac{dE_{\rm tot}}{d\rho_0} = 0.$$

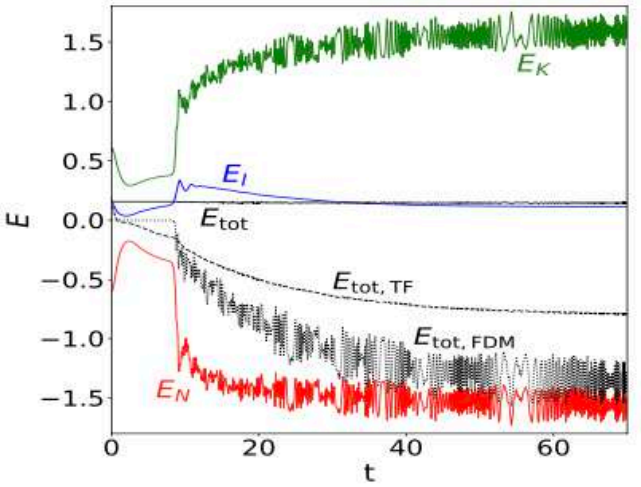

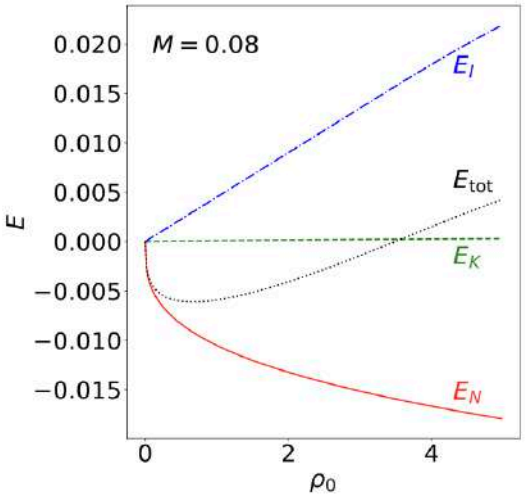

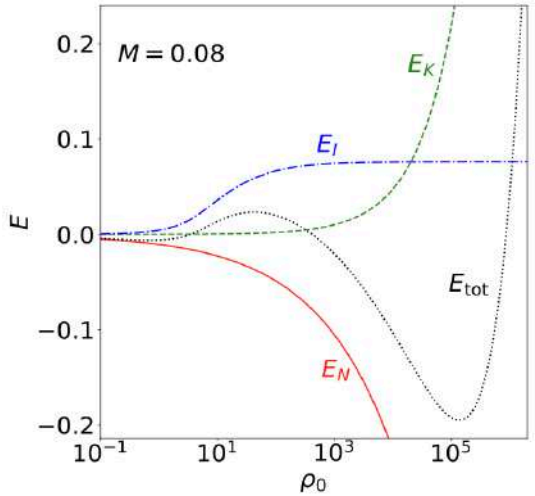

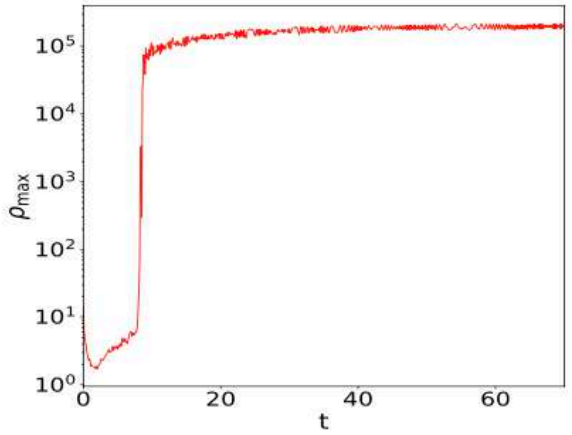

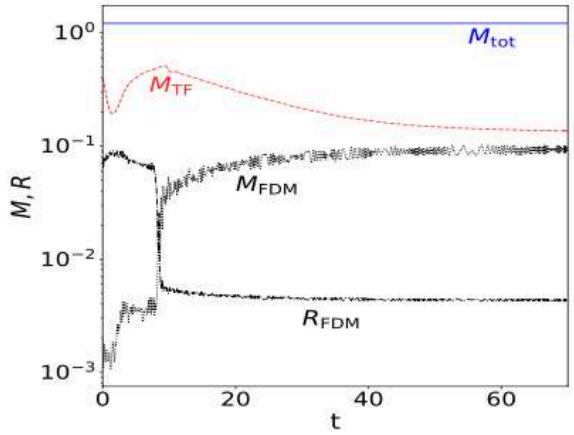

SFDM Motivation: Explanation to CDM small-scales tensions

Missing satellite problem

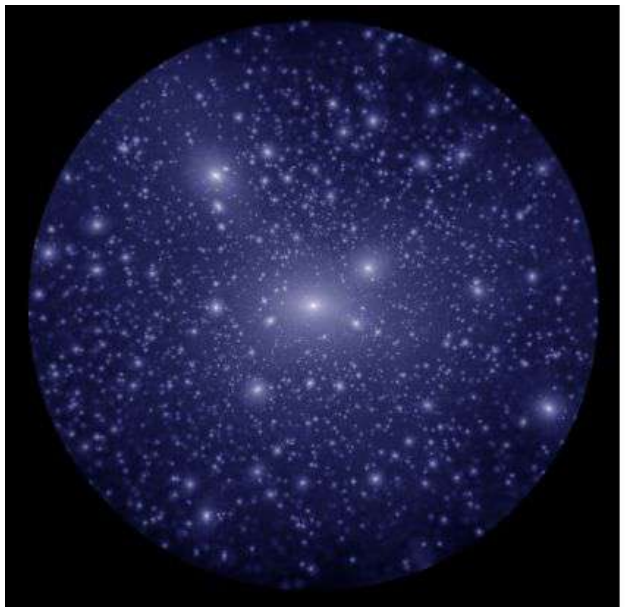

Predicted ΛCDM substructure

Simulation by V. Robles and T. Kelley and collaborators.

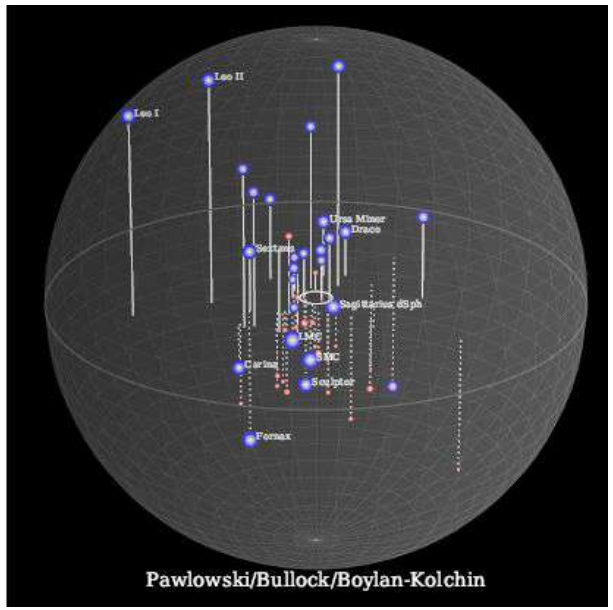

Known Milky Way satellites

James S. Bullock, M. Boylan-Kolchin, M. Pawlowski

Core/cusp problem

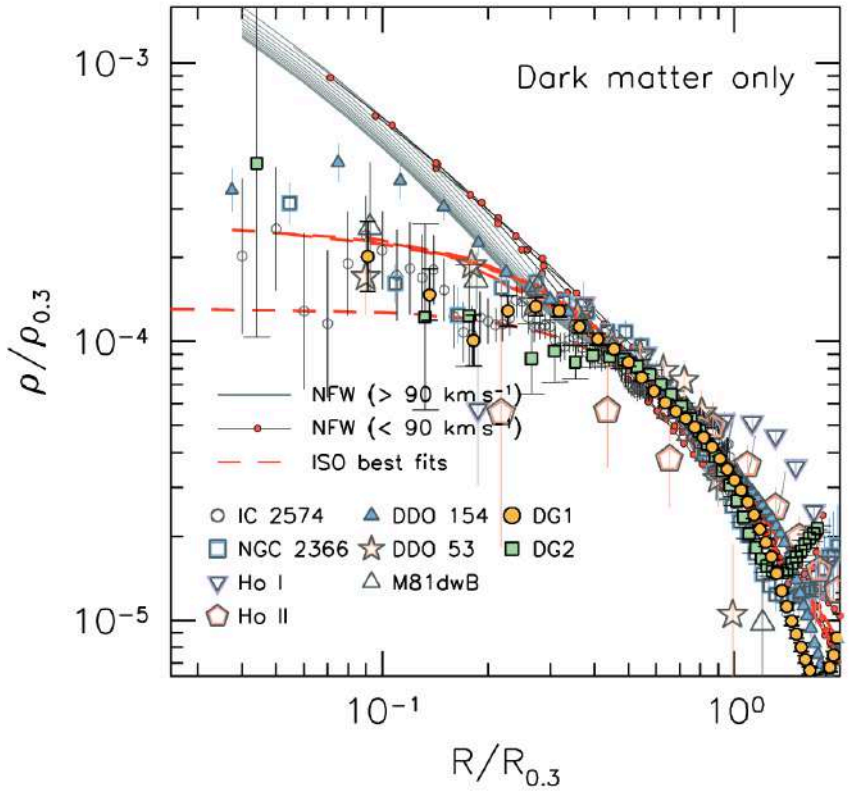

Density profiles observations and simulations

Antonino Popolo, Morgan Le Delliou (2017)

SFDM Motivation 2) Alternative to CDM N-Body simulations

FDM comoving Vlasov equation

$$\frac{\partial f_{\rm W}}{\partial t} + \frac{\vec{p}}{a^2} \cdot \frac{\partial f_{\rm W}}{\partial \vec{x}} - \vec{\nabla}_x \varphi_{\rm N} \cdot \frac{\partial f_{\rm W}}{\partial \vec{p}} + \mathcal{O}(\epsilon) = 0.$$

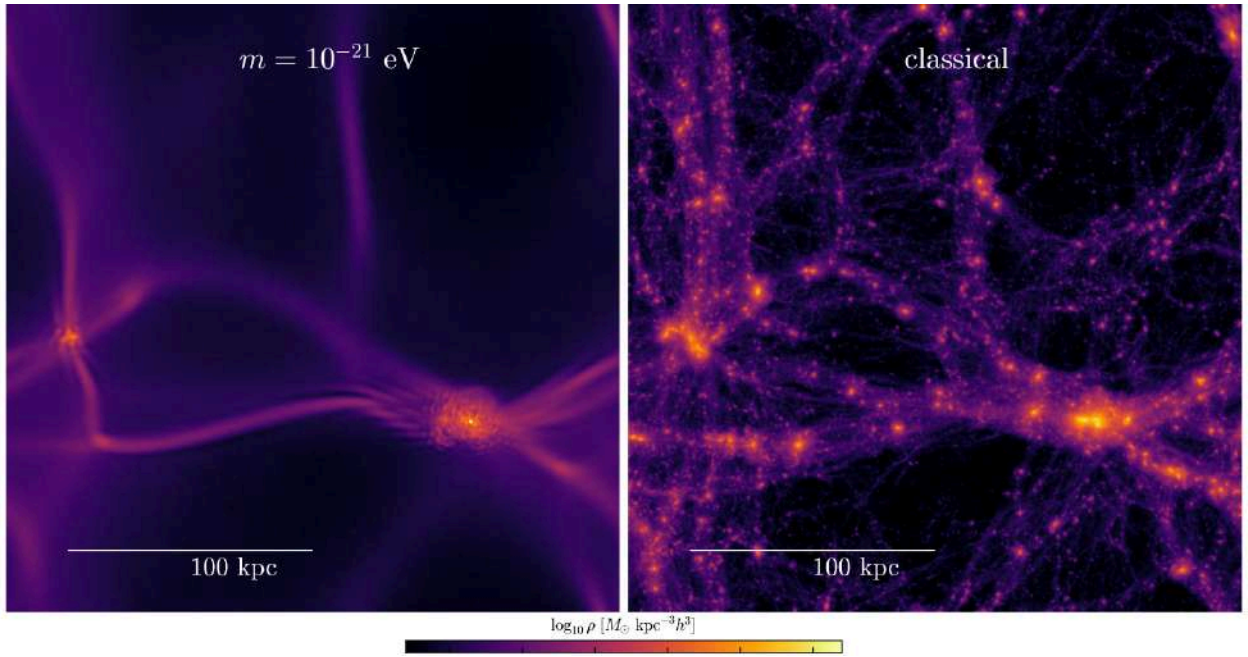

Cosmological simulation at z=3, evolved either as CDM (VP eq) or as FDM (SP)

Philip Mocz and Lachlan Lancaste
Anastasia Fialkov and Fernando Becerra
Pierre-Henri Chavanis (2018).

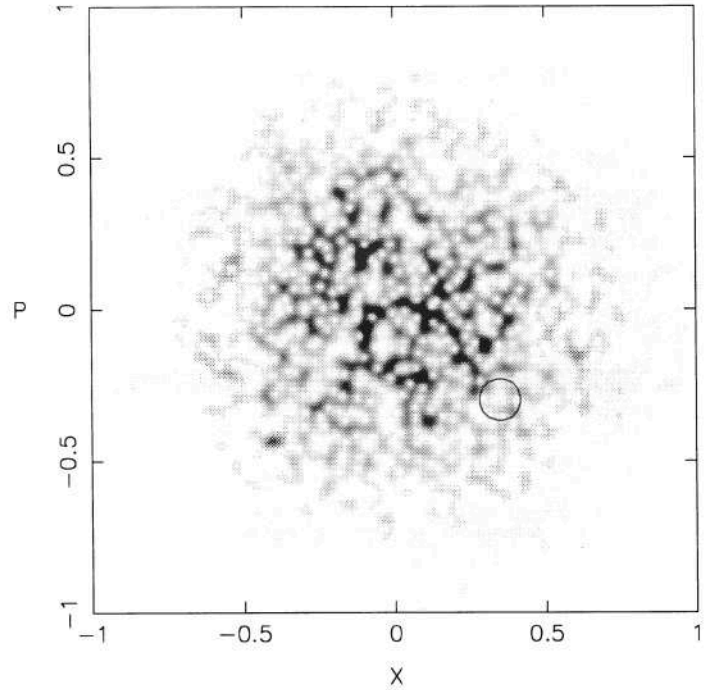

Using Schrodinger equation to compute collisionless cold dark mater
Kaiser (1993)

I) Flat halo with r_a of the order of the system

Density slice *2D (x,y)* **at** $z=r_{max,}$ (ρ_{max})

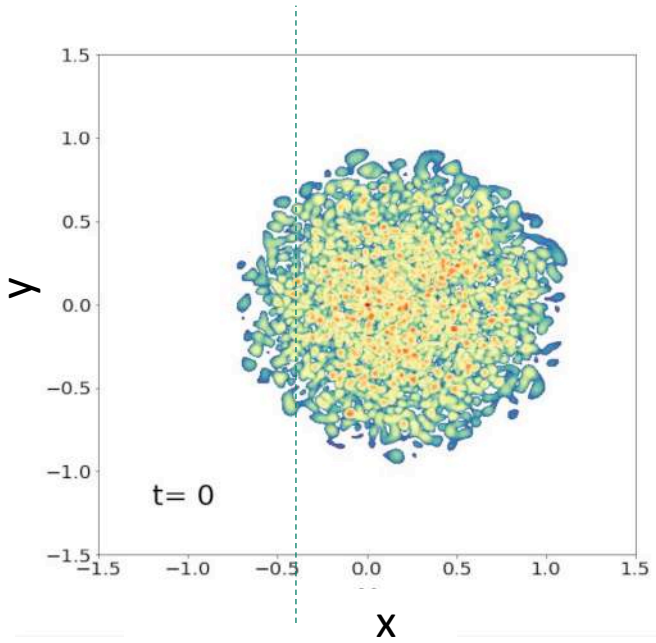

$$R_{\rm sol} = \frac{\sqrt{\lambda\pi}}{2}, = 0.5$$

ρ_{max} , E_K, E_I, E_N

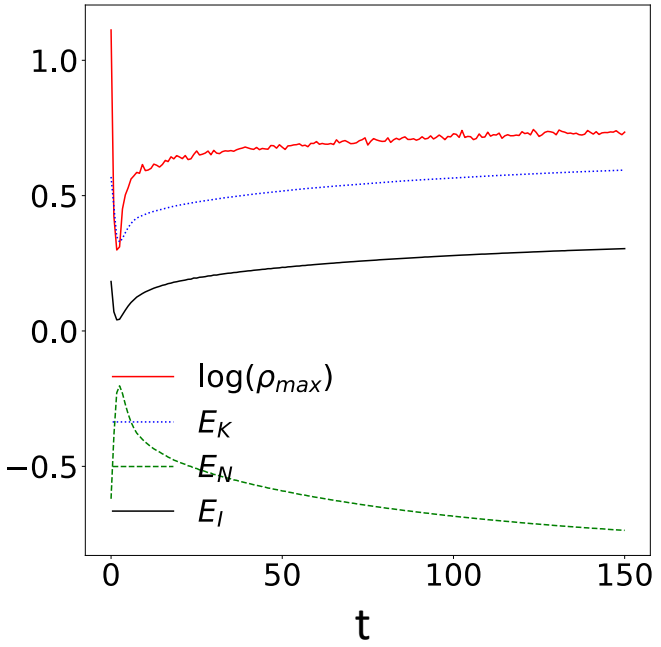

Potential at t=150

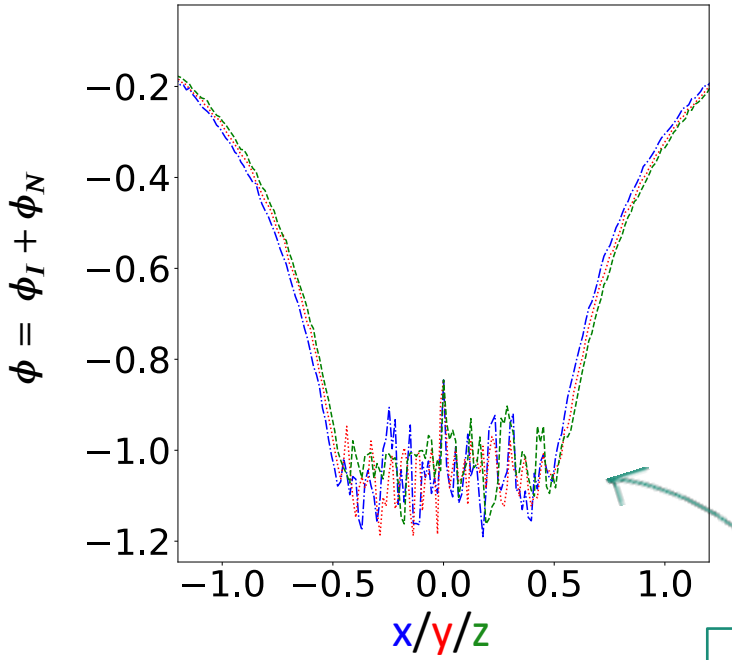

Soliton

$$\Phi_N + \Phi_I = \alpha,$$

- At t ~ 8, the soliton is formed with R_{sol} = 0.5 and contains about 40% of the total mass.
- The system reaches a quasi-stationary state.
- Afterwards, ρ_{max} and the energies only show a slow evolution.

II) Flat halo with r_a much smaller than system

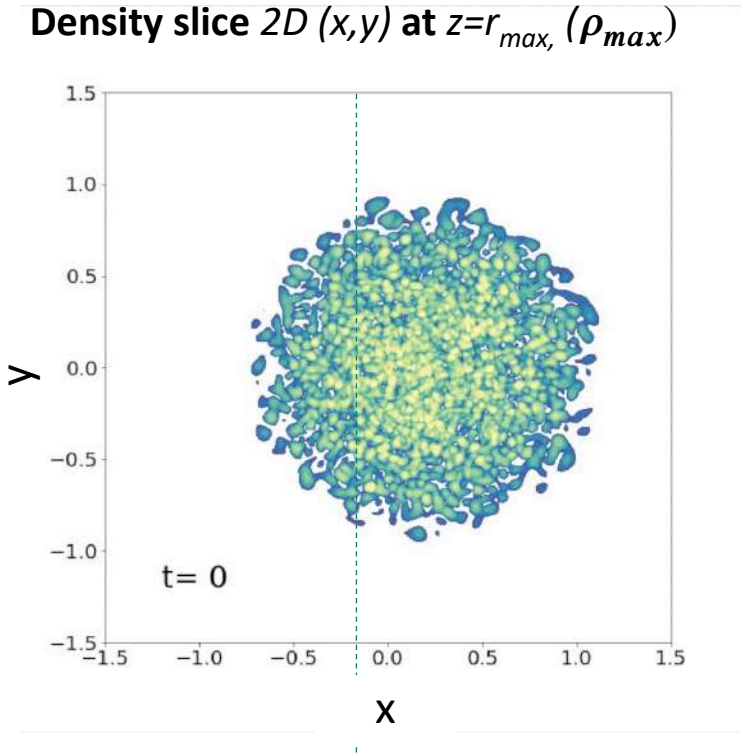

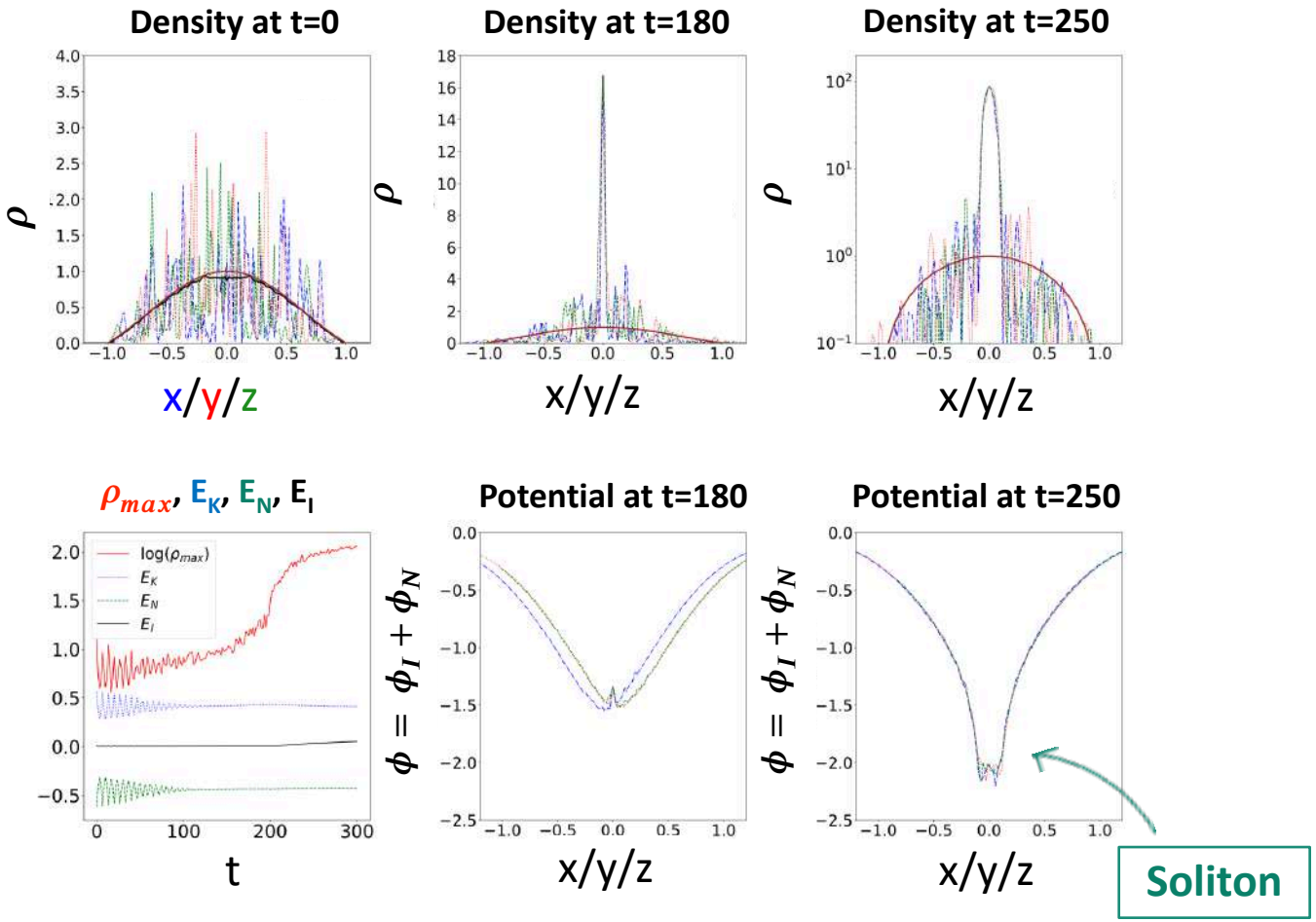

- By t ~ 100, the halo relaxes to a quasi-stationary state.
- At t ~180, FDM peak.
- At t ~ 200, self-interacting soliton forms, R_{sol} = 0.1 .

Transition from a FDM phase to a self-interacting phase.

We focus on an effective model of scalar dark matter that remains valid below a specific cut-off energy scale, denoted as Λ

where $V_I(\phi)$ is the self-interaction potential,

$$V_I(\phi) = \Lambda^4 \sum_{n\geq 3} \frac{\lambda_p}{p} \frac{\phi^p}{\Lambda^p}.$$

$$\phi = \frac{1}{\sqrt{2m}}(\psi e^{-imt} + \psi^* e^{imt}), \tag{2.33}$$

This allows us to separate the fast oscillations at frequency $m \sim (3 \text{ months})^{-1}$ from the slower dynamics described by ψ that follow the evolution of the density field and of the gravitational potential. Note that the complex scalar field ψ also satisfies the slow varying conditions (2.28)-(2.29), that is, $\dot{\psi} \ll m\psi$ and $\nabla\psi \ll m\psi$. Replacing (2.33) into the Klein-Gordon equation for ϕ (2.31) leads to the Schrödinger equation for ψ,

$$i\frac{\partial\psi}{\partial t} = -\frac{1}{2m}\nabla^2\psi + m\Phi_{\rm N}\psi + \frac{\partial\mathcal{V}_{\mathcal{I}}}{\partial\psi^*}\,, \tag{2.34}$$

where now $\Phi_{\rm N}$ is the gravitational potential. Note that we have changed the notation from $\Phi \to \Phi_{\rm N}$. The self-interaction potential, denoted as $\mathcal{V}_{\mathcal{I}}(\psi, \psi^*)$ is derived by replacing the decomposition (2.33) in the definition of $V_I(\phi)$, (2.3). We selectively keep only the non-oscillatory terms. This implies that in the series expansion (2.3), we exclusively consider the even order terms ϕ^{2n}, where each n factor of e^{-imt} is paired with n factors of e^{imt}. Consequently, the resulting expression is:

$$\mathcal{V}_{\mathcal{I}}(\psi, \psi^*) = \Lambda^4 \sum_{n=2} \frac{\lambda_{2n}}{2n} \frac{(2n)!}{(n!)^2} \left(\frac{m\psi\psi^*}{2m\Lambda^2} \right)^n . \tag{2.35}$$

Next, let us define the following self-interaction potential to make the Schrödinger equation (2.34) more user-friendly,

$$\Phi_{\rm I}(\rho) = \frac{d\mathcal{V}_{\mathcal{I}}}{d\rho}, \tag{2.36}$$

where ρ is the ultra-light scalar density,

$$\rho = m\psi\psi^*. \tag{2.37}$$

Field picture

- Relativistic regime + FLRW background:

$$\ddot{\phi} + 3H(t)\dot{\phi} + \frac{dV(\phi)}{d\phi} = 0,$$

- The Einstein-Klein Gordon system.
- The non-relativistic regime relevant for structure formation, it is useful to introduce a complex scalar ψ

$$\phi = \frac{1}{\sqrt{2ma^3}}(\psi e^{-imt} + \psi^* e^{imt}),$$

$\left|\ddot{\psi}\right| \ll m\left|\dot{\psi}\right|$ Factor-out the fast time oscillation of ϕ

Field picture: Schrodinger—Poisson system (SP)

The equations of motion of the action yield the Nonlinear Schrödinger—Poisson system:

$$i\dot{\psi} = -\frac{3}{2}iH\psi - \frac{1}{2ma^2}\nabla^2\psi + m(\Phi_{\rm N} + \Phi_{\rm I}),$$

$$\nabla^2\Phi_{\rm N} = 4\pi G m a^2 |\psi|^2.$$

At small-scales, expansion of the universe is negligible:

$$i\frac{\partial\psi}{\partial t} = -\frac{1}{2m}\nabla^2\psi + m(\Phi_{\rm N} + \Phi_{\rm I})\,\psi,$$

$$\nabla^2\Phi_{\rm N} = 4\pi\mathcal{G}_{\rm N}\rho.$$

$$\rho = m\psi\psi^*.$$

Mass limits

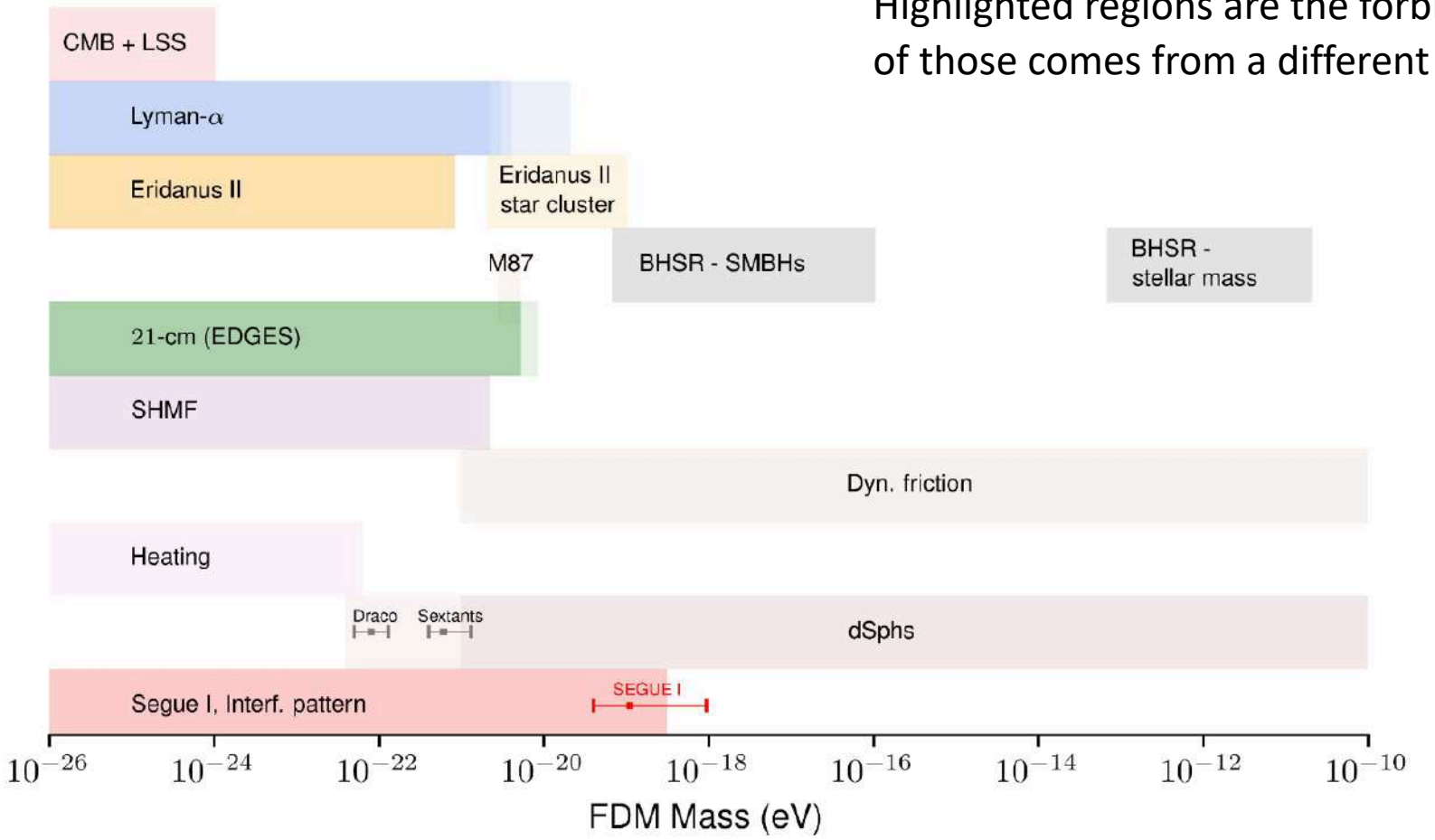

Highlighted regions are the forbidden regions for the mass each of those comes from a different observation

Cosmological evolution

Cosmological evolution

Slide: Elisa M Ferreira
Cosmology from home
2022

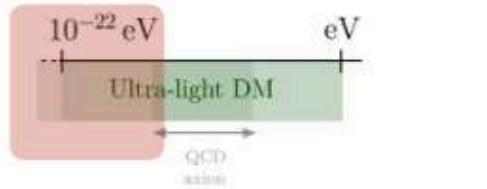

$$\ddot{\phi} + 3H\dot{\phi} + m^2\phi = 0 \qquad \text{FDM}$$

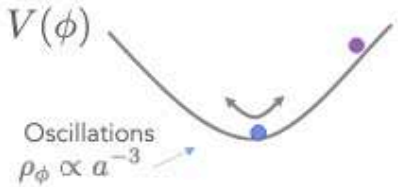

$$\begin{cases} H \gg m \implies \phi_{\text{early}} = \phi(t_i) \longrightarrow \omega = -1 & \text{DE} \\ H \ll m \implies \phi_{\text{late}} \propto e^{imt} \longrightarrow \langle\omega\rangle = 0 & \text{DM} \end{cases}$$

$$V(\phi) = \Lambda_a^4 [1 - \cos(\phi/f_a)] \to \frac{1}{2}m^2\phi^2 + \frac{g}{4}\phi^4$$

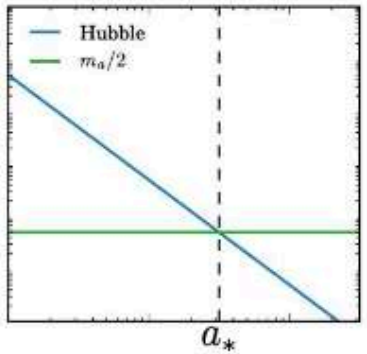

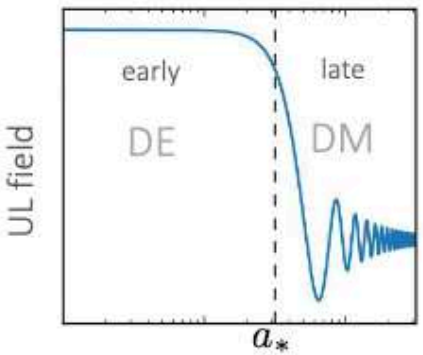

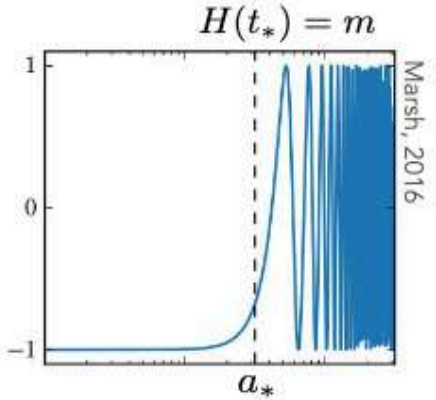

In order to behave like DM: start oscillating before matter-radiation equality $m > 10^{-28}\,\text{eV} \sim H(a_{\text{eq}})$

Structure formation - perturbation and stability

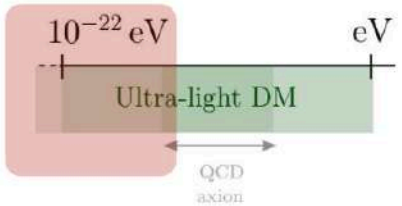

Finite clustering scale - no structure formation on small scales

FDM

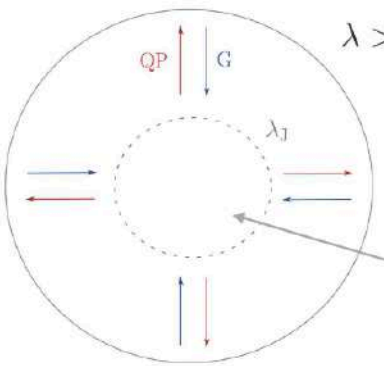

$\lambda > \lambda_J,\ \lambda_{attr},\ \lambda_{rep} \longrightarrow$ CDM

QP wins -
NO structure formation
$\lambda < \lambda_J,\ \lambda_{attr},\ \lambda_{rep}$

Finite size coherent core – Bose stars

$$\lambda_J = 55 \left(\frac{m}{10^{-22}\,\mathrm{eV}}\right)^{-1/2} \left(\frac{\rho}{\bar{\rho}}\right)^{-1/4} (\Omega_m h)^{-1/4}\,\mathrm{kpc}$$

$m \leq 10^{-20}\mathrm{eV} \Rightarrow \lambda_{dB} > \mathcal{O}(\mathrm{kpc})$ Galactic scales

$$\dot{\rho} + \nabla \cdot (\rho\,\mathbf{v}) = 0$$

$$\dot{\mathbf{v}} + (\mathbf{v}\cdot\nabla)\mathbf{v} = -\frac{1}{m}\left(V_{grav} - P_{int} - \frac{1}{2m}\frac{\nabla^2\sqrt{\rho}}{\sqrt{\rho}}\right)$$

$P_{int} = \frac{g}{2m^2}\rho^2$

Quantum pressure

Slide: Elisa M Ferreira
Cosmology from home
2022

Slide: Elisa M Ferreira
Cosmology from home 2022

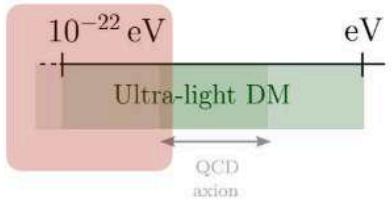

Phenomenology

Suppression of small structures

Finite Jeans length λ_J or $\lambda_{attr}, \lambda_{rep}$ ⟶ Suppresses small scale structure

POWER SPECTRUM

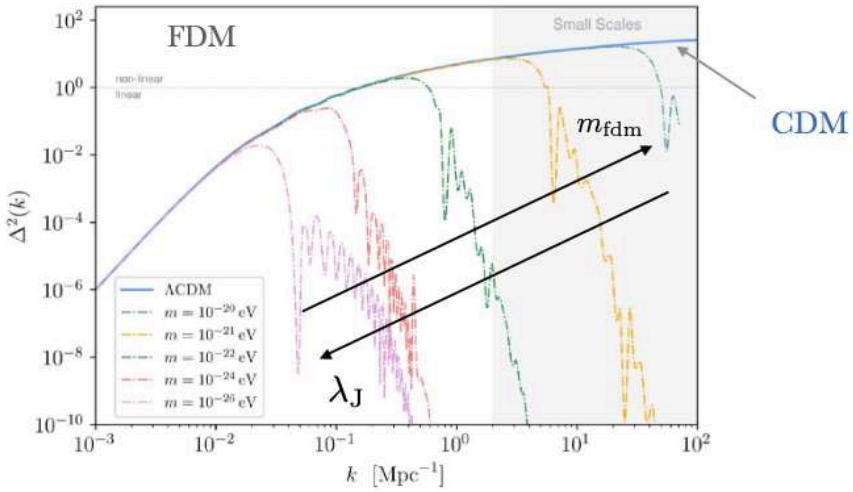

(sub) HALO MASS FUNCTION

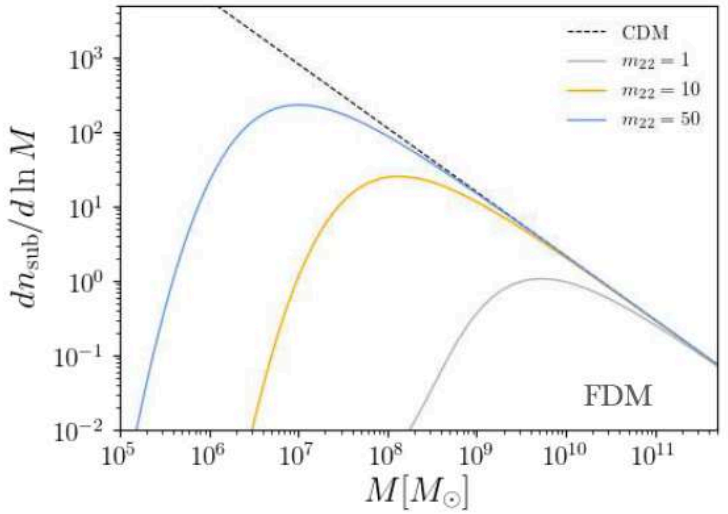

Ultra-light Dark Matter

FDM mass from Ultra-faint dwarfs

Slide: Elisa M Ferreira
Cosmology from home 2022

Hayashi, **E.F**,Chan, 2021.

Ultra-faint dwarfs (UFD): ideal laboratory to study DM

Stellar kinematic data from 18 UFDs to fit the FDM profile:

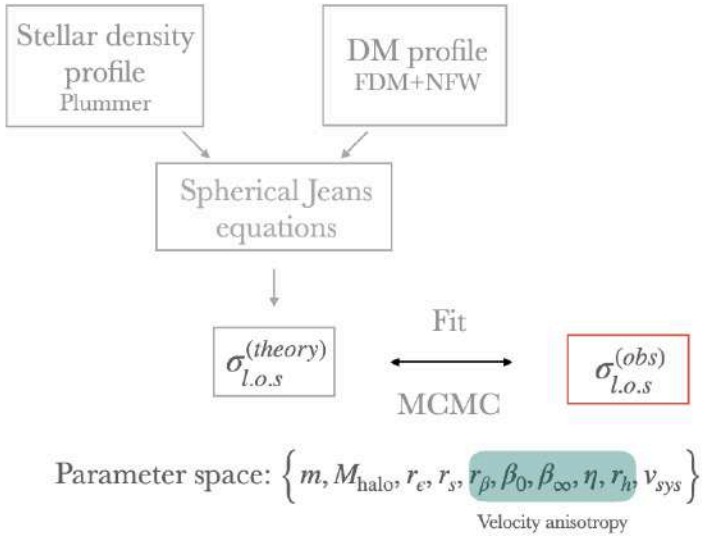

Parameter space: $\{m, M_{\rm halo}, r_e, r_s, r_\beta, \beta_0, \beta_\infty, \eta, r_h, v_{sys}\}$

Velocity anisotropy

FDM SIMULATIONS

$$\rho(r) = \begin{cases} \rho_{\rm soliton} \simeq \dfrac{\rho_c}{\left[1+0.091(r/r_c)^2\right]^8}, & r < r_e \\ \rho_{\rm NFW} = \dfrac{\rho_s}{(r/r_s)(1+r/r_s)^2}, & r > r_e \end{cases}$$

$$\rho_c(r) = 1.9\times10^{12}\left(\frac{m}{10^{-23}\,\mathrm{eV}}\right)^{-2}\left(\frac{r_c}{\mathrm{pc}}\right)^{-4}\ [M_\odot\,\mathrm{pc}]$$

$$r_c \simeq 1600\left(\frac{m}{10^{-23}\,\mathrm{eV}}\right)^{-1}\left(\frac{M_{\rm halo}}{10^{12}\,M_\odot}\right)^{-1/3}\ [\mathrm{pc}]$$

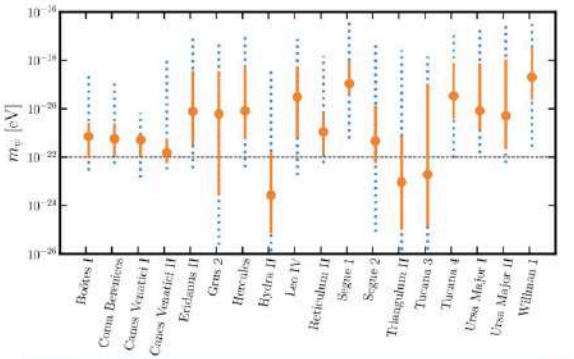

Strongest constraint on $m_{\rm FDM}$ to date!

Particle physics motivations

- A natural candidate for a light (scalar) particle is a pseudo-Nambu-Goldstone boson.

  A well known example is the QCD axion (Peccei, Quinn; Weinberg; Wilczek; Kim; Shifman, Vainshtein, Zakharov, Zhitnitsky; Dine, Fischler, Srednicki; Preskill, Wise, Wilczek; Abbott, Sikivie).

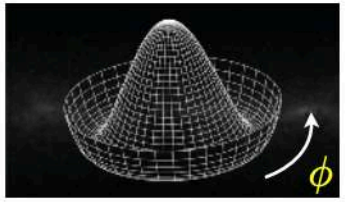

  There are also many axion-like-particles in string theory (Svrcek, Witten; Arvanitaki et al.)

Footnote on ultra -light version

$$\text{mass } m \leftarrow 10^{-22}\,\text{eV} \rightarrow$$

Fuzzy dark matter (FDM)
Hu, Barkana, Gruzinov
Amendola, Barbieri

- Consider an angular field (a pseudo Nambu-Goldstone) of periodicity $2\pi F$ i.e. an axion-like field with a potential from non-perturbative effects (not QCD axion).

$$\mathcal{L} \sim -\frac{1}{2}(\partial\phi)^2 - \Lambda^4(1 - \cos[\phi/F]) \qquad m \sim \Lambda^2/F$$

(candidates: Arvanitaki et al. Svrcek, Witten)

- Relic abundance matches dark matter abundance (mis-alignment mechanism).

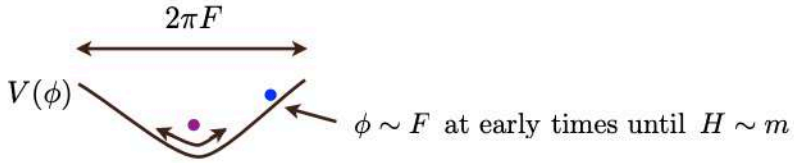

$$\Omega_{\text{matter}} \sim 0.1 \left(\frac{F}{10^{17}\,\text{GeV}}\right)^2 \left(\frac{m}{10^{-22}\,\text{eV}}\right)^{1/2}$$

(Preskill, Wise, Wilczek; Abbot, Sikivie; Dine, Fischler, with constant m)

Slide: Lam Hui
Les Houches Summer School 2021

Experimental implications (light DM e.g. QCD axion):

$$\mathcal{L} \sim \frac{\phi}{f} F_{\mu\nu}\tilde{F}^{\mu\nu} + \frac{\partial_\mu \phi}{f}\bar{\Psi}\gamma^5\gamma^\mu\Psi$$

Reviews: Sikivie 2003
Graham et al. 2015, Marsh 2016

- **Coupling to EM**

  ADMX (cavity) - photon from axion in magnetic field ϕ^2

  ABRACADABRA - magnetic flux from axion in magnetic field $\dot{\phi}$

  ADBC - rotation of polarization of photon propagating in axion $\Delta\phi$

- **Coupling to spin** $\hat{H} \sim \vec{\nabla}\phi \cdot \hat{\sigma}$

  CASPEr - spin precession like in NMR $\vec{\nabla}\phi$

  Eot-Wash - torsional spin pendulum $\vec{\nabla}\phi$

- $\phi \sim \psi e^{-imt} + \psi^* e^{imt}$ (slow, fast)

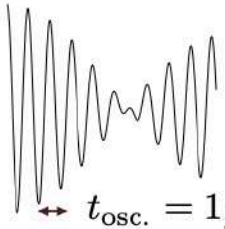

Derevianko; Foster, Rodd, Safdi; Centers et al.

$t_{\rm osc.} = 1/m \sim 10^{-9}\,{\rm s}$

$t_{\rm coherent} = 1/(m\,v^2) \sim 10^{-3}\,{\rm s}$

- Measure correlation functions e.g.
  $\langle\phi(t)^2\phi(t')^2\rangle - \langle\phi^2\rangle^2 \sim [|t-t'|/t_{\rm coherent}]^{-3} + \text{osc.}$ (or even space-time correlations).
- At vortices $\phi = 0$ but $\vec{\nabla}\phi \neq 0$.
- Phase of oscillation might be interesting: $\phi \sim |\psi|\cos(mt-\theta)$.

Slide: Lam Hui
Les Houches Summer School 2021

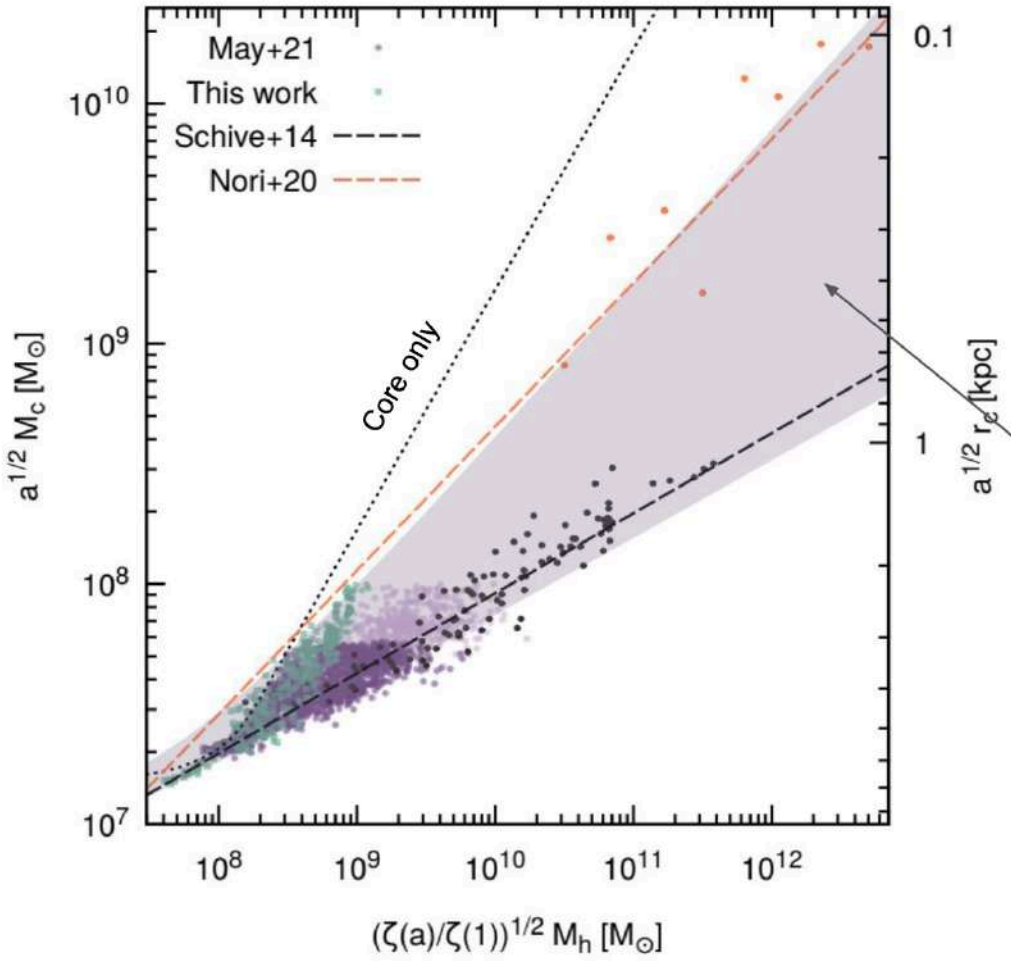

- **Dispersion !**
- **Previous studies only describe part of the core-halo population**

- **New Empirical Equation**

$$M_c = \beta + (M_h/\gamma)^{\alpha}$$

In Schive et al. (2014b), a fitting function for the core–halo mass relation was obtained:

$$M_{\rm c} = \frac{1}{4\sqrt{a}} \left[\left(\frac{\zeta(z)}{\zeta(0)} \right)^{1/2} \frac{M_{\rm h}}{M_{\rm min,0}} \right]^{1/3} M_{\rm min,0}\,, \tag{11}$$

where $M_{\rm c}$ and $M_{\rm h}$ are again the core and halo masses, and $M_{\rm min,0} \sim 4.4 \times 10^7 \left(mc^2/(10^{-22}\,{\rm eV})\right)^{-3/2} {\rm M}_\odot$, and the outer exponent $\alpha = 1/3$ represents the (logarithmic) slope of the relation $M_{\rm c} \propto M_{\rm h}^{\alpha}$. In order to compare with Schive et al. (2014b), we follow their definition of halo mass $M_{\rm h} = (4\pi r_{\rm h}^3/3)\zeta(z)\rho_{\rm m0}$, where $r_{\rm h}$ is the halo's virial radius, $\rho_{\rm m0}$ is the background matter density and $\zeta \sim 180$ (350) for $z = 0$ (≥ 1).

Previous studies were able to confirm the empirical density profile eqs. (8) and (9) using different simulations. However, they disagree about the form of the core–halo mass relation, calling the validity of eq. (11) obtained by Schive et al. (2014b) into question. Schwabe et al. (2016) performed idealised soliton merger simulations and were unable to reproduce eq. (11). Mocz et al. (2017) used a larger halo sample with simulations of a similar setup and obtained a slope of $\alpha = 5/9$, disagreeing with eq. (11). Mina et al. (2020) found the same slope of $5/9$ using cosmological simulations with a box size of $2.5\,{\rm Mpc}\,h^{-1}$. Finally, Nori & Baldi (2021) performed zoom-in simulations by including an external quantum pressure term in an N-body code, and obtained a relation with yet another value of the slope, $\alpha = 0.6$. Such disagreement between different studies indicates that there is still a fundamental lack of understanding of the core–halo structure in the FDM model, and also generates uncertainty in any constraints on the FDM mass which were obtained using eq. (11) or similar relations. Therefore, the main motivation of this work is to